Unifying the Theory of Mutual Coupling Compensation in Antenna Arrays

Simon Henault and Yahia M. M. Antar

Department of Electrical and Computer Engineering, Royal Military College of Canada,
Kingston, ON K7K 7B4, Canada
E-mail: henault@ieee.org

Abstract

The limitations of current mutual coupling compensation methods in antenna arrays are thoroughly reviewed. The theory of mutual coupling compensation is unified in such a way that efficient methods can be employed for calibrating both transmit and receive systems having arbitrary geometries. The theory leads to methods that can evaluate mutual coupling using either theoretical or experimental means. Reciprocity is studied through the careful comparison of receive and transmit analytical formulations. Examples involving various applications are presented for the validation of the theory. This theory has numerous applications and contributes to the areas of antenna theory, mutual coupling analysis, complex structure modeling, and antenna measurements.

Keywords: Antenna arrays; mutual coupling; calibration; direction of arrival (DOA) estimation; beam steering; reciprocity; retrodirective arrays

1. Introduction

Antenna arrays are employed in a variety of applications, including direction of arrival (DOA) estimation, multiple-input multiple-output, beam steering, and interference suppression. In many cases, accurate characterization of the array response is critical in the optimization of the array performance. In particular, the increasing use of arrays that consist of relatively small numbers of closely spaced antenna elements or arrays that are located in the vicinity of scatterers justifies the requirement for mutual coupling compensation. In such systems, electromagnetic coupling between the array elements and scatterers results in nonuniform electromagnetic responses from each of the array elements and degraded performance if mutual coupling compensation is not performed properly.

Mutual coupling compensation can be performed either by the prediction of received or transmitted signals for a given excitation or by a matrix multiplication with the received signals, which restores the signals that would be received in the absence of mutual coupling.

Digital Object Identifier 10.1109/MAP.2015.2414514
Date of publication: 20 April 2015

As discussed in Section 2 of this paper, various methods have been presented in the literature for compensating mutual coupling in antenna arrays. However, many of them appear to be restricted to specific array and element geometries, very often azimuth-only systems involving vertical thin wire array elements. Those that are applicable to systems of arbitrary geometries appear to require excessive amounts of measurements, calculations, and memory. Unfortunately, no work has bridged the gap between efficient mutual coupling compensation methods and those that are applicable to systems of arbitrary geometries. This paper proposes to do so by unifying the theory of mutual coupling compensation.

Going back to the basics of antenna theory in Section 3, useful analytical formulations will be derived as theoretical foundations for unifying the theory. Both receive and transmit antenna systems will be considered, and clear reciprocity relationships relating the two operating modes will be highlighted, giving new guidelines on mutual coupling compensation in a system using data obtained for an operating mode different from its intended one. Techniques for improving mutual coupling compensation efficiency will be presented in Section 4, and various applications of the theory will be described in Section 5.

This paper has potential value as both a review and a tutorial paper and also presents new material. The numerical

examples can be easily verified with proven electromagnetic computational codes. The use of receive-mode mutual coupling compensation data in all examples, even when the systems are employed in transmission, is deliberate as mutual coupling compensation is often performed using receive-mode measurements, and it provides additional validation opportunities.

2. Background

It was recently observed in [1] that although very different coupling mechanisms for transmit and receive systems have existed for quite some time in the literature, many researchers still prefer to analyze receive systems using concepts that better characterize transmit systems. More specifically, array analysis is very commonly performed using the concept of mutual impedances. Let us consider an antenna array of N radiating elements. The mutual impedance between the ith array element $(i = 1, \ldots, N)$ and the jth array element $(j = 1, \ldots, N)$ is determined as

$$Z_{ij} = \frac{V_i}{I_j} \tag{1}$$

where V_i is the voltage appearing at the open-circuited port of element i due to the current source I_j at the port of element j while all the other elements are open-circuited. The impedance matrix is formed using all the mutual impedances as follows:

$$Z = \begin{bmatrix} Z_{11} & Z_{12} & \cdots & Z_{1N} \\ Z_{21} & Z_{22} & \cdots & Z_{2N} \\ \vdots & \vdots & \ddots & \vdots \\ Z_{N1} & Z_{N2} & \cdots & Z_{NN} \end{bmatrix}. \tag{2}$$

Alternatively, the mutual admittances can be determined using

$$Y_{ij} = \frac{I_i}{V_j} \tag{3}$$

where I_i is the current appearing at the short-circuited port of element i due to the voltage source V_j at the port of element j while all the other ports are short-circuited. The impedance matrix is then obtained by

$$Z = Y^{-1}. \tag{4}$$

It is also possible to measure the scattering matrix using a vector network analyzer by making sure that the ports are terminated properly into a reference impedance Z_o commonly having a value of 50 Ω. The impedance matrix is then obtained by

$$Z = Z_o(I_N + S)(I_N - S)^{-1} \tag{5}$$

where S is the scattering matrix, and I_N is the identity matrix having dimensions equal to the number of array elements N. The port voltages are then given by

$$\begin{bmatrix} V_1 \\ V_2 \\ \vdots \\ V_N \end{bmatrix} = \begin{bmatrix} Z_{11} & Z_{12} & \cdots & Z_{1N} \\ Z_{21} & Z_{22} & \cdots & Z_{2N} \\ \vdots & \vdots & \ddots & \vdots \\ Z_{N1} & Z_{N2} & \cdots & Z_{NN} \end{bmatrix} \begin{bmatrix} I_1 \\ I_2 \\ \vdots \\ I_N \end{bmatrix}. \tag{6}$$

Using array theory, the excitation currents required to steer the array radiation pattern in a desired direction are proportional to

$$\begin{bmatrix} I_1 \\ I_2 \\ \vdots \\ I_N \end{bmatrix} = \begin{bmatrix} e^{-\mathrm{j}\frac{2\pi}{\lambda}[\sin\theta_o(x_1\cos\phi_o + y_1\sin\phi_o) + z_1\cos\theta_o]} \\ e^{-\mathrm{j}\frac{2\pi}{\lambda}[\sin\theta_o(x_2\cos\phi_o + y_2\sin\phi_o) + z_2\cos\theta_o]} \\ \vdots \\ e^{-\mathrm{j}\frac{2\pi}{\lambda}[\sin\theta_o(x_N\cos\phi_o + y_N\sin\phi_o) + z_N\cos\theta_o]} \end{bmatrix} \tag{7}$$

where λ is the wavelength of the signal; x_i, y_i, and z_i are the physical coordinates of element i; and ϕ_o and θ_o are the azimuth and elevation angles describing the direction in which the radiation pattern is steered. The impedance seen at port i is the ratio

$$Z_{D_i} = \frac{V_i}{I_i}. \tag{8}$$

Using (6), (7), and (8) yields

$$\begin{aligned} Z_{D_i} &= \sum_{j=1}^{N} Z_{ij}\frac{I_j}{I_i} \\ &= \sum_{j=1}^{N} Z_{ij} e^{\mathrm{j}\frac{2\pi}{\lambda}\left\{\sin\theta_o\left[(x_i - x_j)\cos\phi_o + (y_i - y_j)\sin\phi_o\right] + (z_i - z_j)\cos\theta_o\right\}}. \end{aligned} \tag{9}$$

This impedance is known as the active driving impedance [2] or scan impedance [3]. In the absence of mutual coupling, it is simply equal to the self-impedance, i.e., $Z_{D_i} = Z_{ii}$, and is independent of the element excitations. However, in the presence of mutual coupling, (9) indicates that the active driving impedances are dependent on the element excitations and will vary as the radiation pattern is scanned in various directions. The impedances of the array elements can then only be matched for a given direction. It is possible that the radiated or received power is significantly reduced when scanning in other directions while the generator or load impedances remain fixed. Ultimately, it may even yield to a phenomenon known as scan blindness at angles where the impedance mismatches result in no power being radiated or received. It should be pointed out however that scan blindness implies that all the active driving impedances of the array are purely imaginary. This is generally only possible in infinite regular arrays [2–5] of identical elements since all the elements have to experience similar electromagnetic interactions. Many

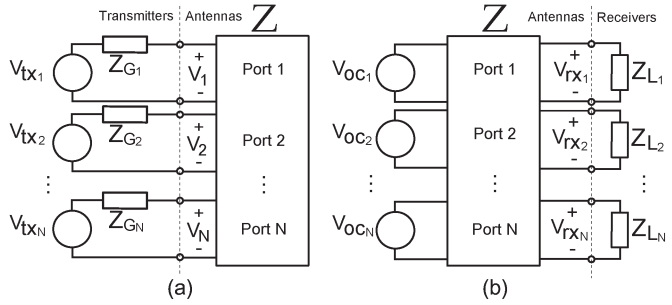

Figure 1. Equivalent circuits of (a) transmit and (b) receive antenna systems.

antenna arrays do not satisfy this condition, and (7)–(9) are therefore of little use in the evaluation of electromagnetic coupling in systems of arbitrary geometries.

The impedance matrix given in (2), however, is very useful in the analysis of these systems. In a transmit system, the impedance matrix is easily integrated in an equivalent circuit, as illustrated in Figure 1a. Voltages $v_{tx_1}, \ldots, v_{tx_N}$ and generator impedances $Z_{G_1}, \ldots, Z_{G_N}$ can be arranged into column vector $\mathbf{v}_{tx}$ and diagonal matrix Z_G to model a set of applied transmitters, which are connected in series with matrix Z that models the antenna array. By circuit theory, the port currents and voltages can be determined based on knowledge of the transmitter voltages, i.e.,

$$\mathbf{I} = (Z_G + Z)^{-1}\mathbf{v}_{tx} \tag{10}$$

$$\mathbf{v} = Z\mathbf{I} = Z(Z_G + Z)^{-1}\mathbf{v}_{tx} \tag{11}$$

where column vectors $\mathbf{I}$ and $\mathbf{v}$ contain the port currents and voltages, respectively. In a receive system as illustrated in Figure 1b, voltages $v_{oc_1}, \ldots, v_{oc_N}$ can be arranged into column vector $\mathbf{v}_{oc}$ to model the antenna array with matrix Z, and load impedances $Z_{L_1}, \ldots, Z_{L_N}$ can be arranged into diagonal matrix Z_L to model a set of attached receivers. Port voltages $v_{rx_1}, \ldots, v_{rx_N}$ are measured across the load impedances by the set of receivers, and these voltages can be arranged into column vector $\mathbf{v}_{rx}$. While the determination of the port quantities is very straightforward in transmit systems since the generator signals can be precisely controlled, it is significantly more complicated in receive systems. In fact, the determination of $\mathbf{v}_{oc}$ due to an external illumination is very rarely encountered in the literature [6–9], and often, crude approximations of the current distributions on the antennas are employed in its calculation [10–14]. This may have contributed to controversies about the validity of the equivalent circuit in Figure 1b [15–21]. However, the fundamental principles already found in classical textbooks [22–24] and reviewed in [25] were verified in [26–28]. The equivalent circuit is valid as long as we are interested only in the port quantities. More specifically, using this circuit for determining the scattered fields would be misleading.

An important limitation of the equivalent circuits in Figure 1 is that they only model systems at the circuit level and give very limited insight about radiated electromagnetic fields. This limitation is generally circumvented through the use of the active element patterns [29–33]. These are also referred to as embedded element patterns [34] or scan element patterns [3]. They are essentially the radiation patterns of the individual elements when these are excited while the other elements are terminated. In [35–39], the definition was modified to the radiation patterns of the individual elements when these are excited while the other elements are open circuited. A limitation of all these active element pattern analysis methods is that they are only accurate in directions for which the radiation patterns are known. Since the radiation patterns are determined for a discrete number of directions relative to the antenna system, some form of interpolation, as suggested in [40–45], can be employed to estimate the radiation patterns in intervening directions. Nevertheless, a large memory requirement can be expected for these methods to store the radiation patterns and obtain good angular resolution.

Analysis methods based on the concept of coupling matrices can potentially minimize this memory requirement. These are only employed in receive systems in the literature [46]. The main assumption of these methods is that the port voltages are related to the incident signals according to

$$\mathbf{v}_{rx}(\phi, \theta) = C\mathbf{v}_{ideal}(\phi, \theta) \tag{12}$$

where

$$C = \begin{bmatrix} C_{11} & C_{12} & \cdots & C_{1N} \\ C_{21} & C_{22} & \cdots & C_{2N} \\ \vdots & \vdots & \ddots & \vdots \\ C_{N1} & C_{N2} & \cdots & C_{NN} \end{bmatrix} \tag{13}$$

$$\mathbf{v}_{ideal}(\phi, \theta) = \begin{bmatrix} e^{j\frac{2\pi}{\lambda}[\sin\theta(x_1\cos\phi + y_1\sin\phi) + z_1\cos\theta]} \\ e^{j\frac{2\pi}{\lambda}[\sin\theta(x_2\cos\phi + y_2\sin\phi) + z_2\cos\theta]} \\ \vdots \\ e^{j\frac{2\pi}{\lambda}[\sin\theta(x_N\cos\phi + y_N\sin\phi) + z_N\cos\theta]} \end{bmatrix}. \tag{14}$$

The matrix C is known as the coupling matrix and contains the complex coupling parameters C_{ij} between elements i and j. Column vectors $\mathbf{v}_{rx}(\phi, \theta)$ and $\mathbf{v}_{ideal}(\phi, \theta)$ contain the port voltages and the incident signals, respectively, and ϕ and θ are the azimuth and elevation angles of the incident signals. The vector $\mathbf{v}_{ideal}(\phi, \theta)$ contains the relative voltages that would appear at the ports under ideal conditions with no mutual coupling present; the voltages are directly proportional to the incident electric fields at the locations of the ports given by x_i, y_i, and z_i in (14). Although the independence of the coupling matrix from the incident angles is often questioned in the literature [47–49], it is generally agreed that for a simple azimuth-only system comprised of vertical wire elements, the coupling matrix is completely independent of the incident direction. This has the practical advantage of completely modeling this type of receive system using a

square matrix whose dimensions are equal to the number of elements.

Unlike active element pattern methods that perform mutual coupling compensation through the prediction of received signals, this method allows compensation to be performed through a matrix multiplication with the received signal vector as follows:

$$\mathbf{v}_{ideal}(\phi,\theta) = C^{-1}\mathbf{v}_{rx}(\phi,\theta). \tag{15}$$

This restores the signals that would be received in the absence of mutual coupling [49] and is a desirable feature for many DOA estimation and radiation pattern synthesis algorithms that rely on specific array geometries.

Various methods have been proposed for the estimation of the coupling matrix. The most popular of these is generally referred to as the open-circuit voltage method and has been used in [50–56]. This method assumes that the coupling matrix is simply given by

$$C = Z_L(Z_L + Z)^{-1}. \tag{16}$$

Therefore, it is implicitly assumed that the open-circuit voltages $\mathbf{v}_{oc}$ in Figure 1b are free from mutual coupling. This is, in general, incorrect, as pointed out in [8, 9, 57]. The assumption is only valid for arrays of electrically small elements in the absence of external scatterers. The full-wave method was introduced in [57] to improve the estimation of C for more common array elements, namely, vertical half-wave dipoles. This was done by judiciously summing up the entries of the method of moments [58] admittance matrix to give a square matrix. A generalization of this method to arbitrary numerical techniques was presented in [8, 9] and gives similar accuracy. Although very accurate, a limitation of the method is that the elevation angle θ of incident signals needs to be known *a priori*. Furthermore, it is better suited to theoretical evaluation. Depending on the complexity of the antenna system at hand, it is sometimes preferable to perform experimental estimation of the coupling matrix. The calibration method employed in [59–61] facilitates experimental estimation by mapping measured vectors to ideal vectors in a least squares sense for several incident directions, resulting in a square coupling matrix estimate. A disadvantage of this method is that a large number of measurements may be required to obtain an accurate estimate. The receiving mutual impedance method was more recently used in [62–66], where, instead of determining the mutual impedances by exciting the elements at their ports as conventionally done, the mutual impedances are determined by exciting the elements by external plane waves. Although this method has the practical advantage of being suitable to experimental implementation, it cannot be expected to provide an accurate estimate of the coupling matrix for arbitrary frequencies and array configurations due to the assumptions that the current distributions on the elements remain unchanged by the elevation angle, the presence of more than two elements in the array, and the azimuth angle of the exciting plane wave used in the determination of the mutual impedances [67]. Nevertheless, it proved to be superior to the conventional open-circuit voltage method in typical configurations of vertical half-wave dipoles.

All the previous coupling matrix estimation methods are considered to be offline methods as they evaluate electromagnetic coupling prior to the operation of the antenna system. Online methods can also be found in the literature [68–78] and are also known as autocalibration, self-calibration, or blind-calibration methods. These methods estimate the coupling matrix on a continuous basis during the operation of the antenna system using signals in the environment and have the practical advantage of adapting to a changing electromagnetic environment, which is a difficult problem when the antenna system is located near potential scatterers. A minimum number of signals from different incident directions is required for obtaining a reliable estimate, with some methods requiring as few as one [71] but with the drawback of only being applicable to uniform circular arrays. Unfortunately, all online methods appear to be limited to specific array geometries with most being applicable to uniform linear arrays. This allows the exploitation of the Toeplitz structures of the coupling matrices. However, as pointed out in [79], this inherently imposes very important constraints with respect to the symmetry of the antenna system, and it is unclear whether online methods can truly adapt to a changing electromagnetic environment since symmetry is lost whenever scatterers approach the system. Furthermore, oversimplifying assumptions are made in all online methods involving uniform linear arrays with respect to the structure of the coupling matrix. Since the elements of this kind of array generally experience dissimilar electromagnetic interactions, it is incorrect to assume constant diagonals, as is the case in a Toeplitz matrix [79]. Only [68] attempted to take this into consideration, but as pointed out in [79], the correction introduced in [68] violates the well-known reciprocity theorem of antenna systems. In light of these important issues, there are serious doubts that online methods can reliably be employed in practical systems.

In [80], it was found that the coupling matrix concept just fails in the presence of structure scattering. More specifically, the experiment consisted of a uniform linear array of vertical dipoles in front of a rectangular conducting plate. The scattering caused by the presence of the conducting plate adversely affected the accuracy of the coupling matrix estimate. Although no solution to this problem was proposed in [80], attempts of a possible solution can be found in [47] and [81–85]. So far, only square coupling matrix estimates have been discussed, and the latter references suggested that under certain conditions, mutual coupling may be better described by nonsquare matrices having a larger number of columns than rows. Instead of summing up the entries of the method of moments admittance matrix as done in the full-wave method in [57], [81–83] used entire rows of the matrix as the coupling matrix estimate. This estimate has the disadvantages of often requiring large memory storage and of being noninvertible due to its nonsquare dimensions. Again, this is

predominantly a theoretical approach, and a more experimental approach can be found in [47], [84], and [85], where measurements were used to estimate a nonsquare coupling matrix. However, these references only considered very specific system geometries and therefore failed to provide a complete approach for the experimental evaluation of mutual coupling.

Although the undesired effects of mutual coupling appear to be unavoidable in practical systems even by careful antenna design [86], a unified theory for the evaluation of mutual coupling and the subsequent compensation of its undesired effects is still missing. The coupling matrix concept appears to be helpful for developing this theory, but a systematic approach needs to be devised to minimize the dimensions of the coupling matrix estimates for systems that are better described by nonsquare matrices. The experimental estimation of these matrices also needs to be generalized with a view to minimizing the number of required measurements. Finally, the evaluation of coupling matrices in transmit systems needs to be studied since coupling matrices have only been used in receive systems. The remainder of this paper achieves this with complete theoretical analysis of receive and transmit systems demonstrated with practical applications of antenna arrays.

3. Theoretical Foundations

3.1 Receive System

Receive quantities of an antenna can be derived using knowledge of *transmit* near-fields $\vec{E}(x,y,z)$ and $\vec{H}(x,y,z)$ for the same reciprocal antenna [87]. By Love equivalence principle [88], equivalent electric and magnetic currents can be formed using

$$\begin{aligned}\vec{J}_{eq} &= \hat{n}\times\vec{H}(x,y,z)\\ \vec{M}_{eq} &= -\hat{n}\times\vec{E}(x,y,z)\end{aligned} \tag{17}$$

where $\hat{n}$ is a unit vector normal to a closed surface enclosing the antenna. This surface has an arbitrary shape but must enclose the antenna completely. To minimize the surface of integration in subsequent equations, however, it is recommended to reduce the shape of the closed surface to that of the antenna. For example, the closed surface enclosing a wire antenna could simply be the metallic surfaces on the wire. By circuit analysis, if the equivalent currents are determined for a unit-voltage source directly at the antenna port, the port voltage when the antenna is excited by an external electromagnetic field is given by

$$v_{rx} = -(Y_L+Y)^{-1}\oint_S(\vec{J}_{eq}\cdot\vec{E}_i - \vec{M}_{eq}\cdot\vec{H}_i)dS \tag{18}$$

where $\vec{E}_i$ and $\vec{H}_i$ are the incident electric and magnetic fields, Y_L and Y are the load and antenna admittances, respectively, and dS is the closed-surface area used in the integration. This equation can be discretized and reformulated as follows:

$$v_{rx} = -\Delta s(Y_L+Y)^{-1}\begin{bmatrix}\mathbf{J_x}\\ \mathbf{J_y}\\ \mathbf{J_z}\\ -\mathbf{M_x}\\ -\mathbf{M_y}\\ -\mathbf{M_z}\end{bmatrix}^T\begin{bmatrix}\mathbf{E_x}\\ \mathbf{E_y}\\ \mathbf{E_z}\\ \mathbf{H_x}\\ \mathbf{H_y}\\ \mathbf{H_z}\end{bmatrix} \tag{19}$$

where $(\cdot)^T$ denotes the transpose operation; Δs is the area of the discretizations assuming that they have the same size; $\mathbf{J}_x$, $\mathbf{J_y}$, $\mathbf{J_z}$, $\mathbf{M_x}$, $\mathbf{M_y}$, and $\mathbf{M_z}$ are column vectors containing the electric and magnetic current x, y, and z components at discrete locations on the closed surface S; and $\mathbf{E_x}$, $\mathbf{E_y}$, $\mathbf{E_z}$, $\mathbf{H_x}$, $\mathbf{H_y}$, and $\mathbf{H_z}$ are column vectors containing the incident electric and magnetic field x, y, and z components at these locations. This can be extended in a straightforward manner to array antennas where multiple ports can be excited. In this case, v_{rx} becomes a column vector instead of a scalar, and the column vectors $\mathbf{J_x}$, $\mathbf{J_y}$, $\mathbf{J_z}$, $\mathbf{M_x}$, $\mathbf{M_y}$, and $\mathbf{M_z}$ become matrices with a number of columns equal to the number of ports. The procedure for estimating a coupling matrix is summarized as follows.

1) Compute the electric and magnetic fields over a closed surface resulting from the excitation of one port by a unit-voltage source while the other ports are short-circuited. The surface should preferably be as small as possible to minimize the number of entries in the coupling matrix and thereby minimize memory requirement and subsequent computations.

2) Compute the equivalent electric and magnetic currents according to (17) from the fields obtained in step 1.

3) Fill a column of matrices J_x, J_y, J_z, M_x, M_y, and M_z with the electric and magnetic currents obtained in step 2.

4) Repeat steps 1–3 for each port.

5) Form the complete coupling matrix estimate with

$$\tilde{C}_{rx} = -\Delta s(Y_L+Y)^{-1}\begin{bmatrix}J_x\\ J_y\\ J_z\\ -M_x\\ -M_y\\ -M_z\end{bmatrix}^T \tag{20}$$

where Y is the array mutual admittance matrix, and Y_L is a diagonal matrix containing the load admittances at the element ports.

The notation $\tilde{C}_{rx}$ is used here for differentiation with the transmit coupling matrix $\tilde{C}_{tx}$ studied in Section 3.2 and the

square coupling matrix of (13). The matrix $\tilde{C}_{rx}$ generally has a nonsquare structure and constitutes a generalization of the coupling matrix to antenna systems of arbitrary geometry and composition. As such, it can be used for compensating mutual coupling accurately and to predict the received port voltages using

$$\mathbf{v}_{rx} = \tilde{C}_{rx}\mathbf{v}_{\mathbf{ideal}} = \tilde{C}_{rx}\begin{bmatrix}\mathbf{E_x}\\ \mathbf{E_y}\\ \mathbf{E_z}\\ \mathbf{H_x}\\ \mathbf{H_y}\\ \mathbf{H_z}\end{bmatrix} \tag{21}$$

where the vector $\mathbf{v}_{rx}$ contains the port voltages. Note that the column vector on the right side of (21) allows for excitations in arbitrary incident directions as well as arbitrary polarizations. The complete response of an array can therefore be predicted using this method.

For plane wave incidence in a lossless isotropic medium, the relation between the incident electrical and magnetic fields is given by

$$\vec{H}_i = -\frac{1}{\eta}\hat{r}\times\vec{E}_i \tag{22}$$

where η is the intrinsic impedance of the propagating medium, and $\hat{r}$ is a unit vector in the radial direction. Carrying out this vector product gives

$$\vec{H}_i = \hat{\theta}\frac{E_\phi}{\eta} - \hat{\phi}\frac{E_\theta}{\eta} \tag{23}$$

where $\hat{\theta}$ and $\hat{\phi}$ are unit vectors in the θ and ϕ directions, respectively, and E_θ and E_ϕ are the θ and ϕ components of the incident electric field in spherical coordinates. Both incident electric and magnetic fields have no radial component. Therefore, they can be modeled in Cartesian coordinates using

$$\begin{aligned}\begin{bmatrix}E_x\\ E_y\\ E_z\end{bmatrix} &= \begin{bmatrix}\cos\theta\cos\phi & -\sin\phi\\ \cos\theta\sin\phi & \cos\phi\\ -\sin\theta & 0\end{bmatrix}\begin{bmatrix}E_\theta\\ E_\phi\end{bmatrix}\\ &= \begin{bmatrix}E_\theta\cos\theta\cos\phi - E_\phi\sin\phi\\ E_\theta\cos\theta\sin\phi + E_\phi\cos\phi\\ -E_\theta\sin\theta\end{bmatrix}\end{aligned} \tag{24}$$

$$\begin{aligned}\begin{bmatrix}H_x\\ H_y\\ H_z\end{bmatrix} &= \begin{bmatrix}\cos\theta\cos\phi & -\sin\phi\\ \cos\theta\sin\phi & \cos\phi\\ -\sin\theta & 0\end{bmatrix}\begin{bmatrix}\frac{E_\phi}{\eta}\\ -\frac{E_\theta}{\eta}\end{bmatrix}\\ &= \begin{bmatrix}\frac{E_\phi\cos\theta\cos\phi+E_\theta\sin\phi}{\eta}\\ \frac{E_\phi\cos\theta\sin\phi-E_\theta\cos\phi}{\eta}\\ -\frac{E_\phi\sin\theta}{\eta}\end{bmatrix}.\end{aligned} \tag{25}$$

The column vector on the right side of (21) then takes the following form:

$$\mathbf{v}_{ideal} = \begin{bmatrix}\mathbf{E}_x\\ \mathbf{E}_y\\ \mathbf{E}_z\\ \mathbf{H}_x\\ \mathbf{H}_y\\ \mathbf{H}_z\end{bmatrix} = \begin{bmatrix}\left(E_\theta\cos\theta\cos\phi - E_\phi\sin\phi\right)\mathbf{v}_i\\ \left(E_\theta\cos\theta\sin\phi + E_\phi\cos\phi\right)\mathbf{v}_i\\ -E_\theta\sin\theta\mathbf{v}_i\\ \frac{E_\phi\cos\theta\cos\phi+E_\theta\sin\phi}{\eta}\mathbf{v}_i\\ \frac{E_\phi\cos\theta\sin\phi-E_\theta\cos\phi}{\eta}\mathbf{v}_i\\ -\frac{E_\phi\sin\theta}{\eta}\mathbf{v}_i\end{bmatrix} \tag{26}$$

where $\mathbf{v}_i = e^{\mathrm{j}(2\pi/\lambda)[\sin\theta(\mathbf{x}\cos\phi+\mathbf{y}\sin\phi)+\mathbf{z}\cos\theta]}$, and the column vectors $\mathbf{x}$, $\mathbf{y}$, and $\mathbf{z}$ contain the x, y, and z coordinates of the discrete locations on the closed surface.

3.2 Transmit System

Well-known manipulations of Maxwell's equations for far-field radiation in a lossless isotropic medium yield the following electric field radiated by an antenna:

$$\vec{E}_{tx} = -\frac{\mathrm{j}\omega\mu}{4\pi}\oint_S\left(\vec{J}_{eq} - \frac{1}{\eta}\hat{r}\times\vec{M}_{eq}\right)\frac{e^{-\mathrm{j}\frac{2\pi}{\lambda}R}}{R}dS \tag{27}$$

where η and μ are the intrinsic impedance and permeability of the medium, $\omega = 2\pi f$ is the angular frequency, $\hat{r}$ is a unit vector in the radial direction, and R is the distance between the sources $\vec{J}_{eq}$ and $\vec{M}_{eq}$ on the closed surface S and an observation point outside this surface. At large distances from the antenna, it is common to assume that the distance R has a negligible impact on the amplitudes in the integrand of (27) and can be treated as a constant. However, it is still important to consider the phase variations in $e^{-\mathrm{j}(2\pi/\lambda)R}$. Knowing that $\hat{r}\times\vec{M}_{eq} = -\hat{\theta}M_\phi + \hat{\phi}M_\theta$, the phase variations are generally taken into consideration using

$$\vec{E}_{tx} = -\frac{\mathrm{j}\omega\mu}{4\pi R}\oint_S\left[\vec{J}_{eq} + \frac{1}{\eta}\left(\hat{\theta}M_\phi - \hat{\phi}M_\theta\right)\right] \times e^{\mathrm{j}\frac{2\pi}{\lambda}[\sin\theta(x\cos\phi+y\sin\phi)+z\cos\theta]}\,dS \tag{28}$$

where M_ϕ and M_θ are the ϕ and θ components of $\vec{M}_{eq}$. The spherical wave propagates in the radial direction $\hat{r}$, and its electric field is orthogonal to this direction. Therefore, $\vec{E}_{tx} = \hat{\theta}E_{tx_\theta} + \hat{\phi}E_{tx_\phi}$ in the far-field, and the radial component of $\vec{J}_{eq}$ in (28) can be ignored. The following expression is then obtained:

$$\vec{E}_{tx} = -\frac{\mathrm{j}\omega\mu}{4\pi R}\oint_S\left[\hat{\theta}\left(J_\theta + \frac{M_\phi}{\eta}\right) + \hat{\phi}\left(J_\phi - \frac{M_\theta}{\eta}\right)\right] \times e^{\mathrm{j}\frac{2\pi}{\lambda}[\sin\theta(x\cos\phi+y\sin\phi)+z\cos\theta]}\,dS. \tag{29}$$

Let the equivalent currents in (29) be those generated by a unit-voltage source at the port of the antenna. If a different

voltage is applied at that port, (29) will scale according to $(Z_G + Z)^{-1} Z v_{tx}$ by circuit theory. For $v_{tx} = 1$V, (29) becomes

$$\vec{E}_{tx} = -\frac{\mathrm{j}\omega\mu}{4\pi R}(Z_G + Z)^{-1} Z \times \oint_S \left[\hat{\theta}\left(J_\theta + \frac{M_\phi}{\eta}\right) + \hat{\phi}\left(J_\phi - \frac{M_\theta}{\eta}\right)\right] \times e^{\mathrm{j}\frac{2\pi}{\lambda}[\sin\theta(x\cos\phi + y\sin\phi) + z\cos\theta]}\, dS. \quad (30)$$

The spherical coordinate quantities J_θ, J_ϕ, M_θ, and M_ϕ are obtained from Cartesian coordinate quantities using the following transformations:

$$\begin{bmatrix} J_\theta \\ J_\phi \end{bmatrix} = \begin{bmatrix} \cos\theta\cos\phi & \cos\theta\sin\phi & -\sin\theta \\ -\sin\phi & \cos\phi & 0 \end{bmatrix} \begin{bmatrix} J_x \\ J_y \\ J_z \end{bmatrix} = \begin{bmatrix} J_x\cos\theta\cos\phi + J_y\cos\theta\sin\phi - J_z\sin\theta \\ -J_x\sin\phi + J_y\cos\phi \end{bmatrix} \quad (31)$$

$$\begin{bmatrix} M_\theta \\ M_\phi \end{bmatrix} = \begin{bmatrix} \cos\theta\cos\phi & \cos\theta\sin\phi & -\sin\theta \\ -\sin\phi & \cos\phi & 0 \end{bmatrix} \begin{bmatrix} M_x \\ M_y \\ M_z \end{bmatrix} = \begin{bmatrix} M_x\cos\theta\cos\phi + M_y\cos\theta\sin\phi - M_z\sin\theta \\ -M_x\sin\phi + M_y\cos\phi \end{bmatrix}. \quad (32)$$

Substituting these quantities into (30) gives

$$\vec{E}_{tx} = -\frac{j\omega\mu}{4\pi R}(Z_G + Z)^{-1} Z \times \oint_S \left[\hat{\theta}\left(J_x\cos\theta\cos\phi + J_y\cos\theta\sin\phi - J_z\sin\theta + \frac{-M_x\sin\phi + M_y\cos\phi}{\eta}\right) + \hat{\phi}\left(-J_x\sin\phi + J_y\cos\phi - \frac{M_x\cos\theta\cos\phi + M_y\cos\theta\sin\phi - M_z\sin\theta}{\eta}\right)\right] \times e^{\mathrm{j}\frac{2\pi}{\lambda}[\sin\theta(x\cos\phi + y\sin\phi) + z\cos\theta]}\, dS. \quad (33)$$

This radiated electric field is seen to consist of two orthogonal components and can be expressed as

$$\vec{E}_{tx} = \hat{\theta}E_{tx_\theta} + \hat{\phi}E_{tx_\phi}. \quad (34)$$

Depending on the polarization of a distant receive system, these two orthogonal components are generally superimposed following a linear combination described by

$$E = E_\theta E_{tx_\theta} + E_\phi E_{tx_\phi} \quad (35)$$

where the scalar parameters E_θ and E_ϕ specify the polarization of the distant receive system. The total electric field at this receive system can then be expressed as

$$E = -\frac{\mathrm{j}\omega\mu}{4\pi R}(Z_G + Z)^{-1} Z \times \oint_S \left[E_\theta\left(J_x\cos\theta\cos\phi + J_y\cos\theta\sin\phi - J_z\sin\theta + \frac{-M_x\sin\phi + M_y\cos\phi}{\eta}\right) + E_\phi\left(-J_x\sin\phi + J_y\cos\phi - \frac{M_x\cos\theta\cos\phi + M_y\cos\theta\sin\phi - M_z\sin\theta}{\eta}\right)\right] \times e^{\mathrm{j}\frac{2\pi}{\lambda}[\sin\theta(x\cos\phi + y\sin\phi) + z\cos\theta]}\, dS. \quad (36)$$

The discrete form of (36) can be expressed as

$$E = -\Delta s\frac{\mathrm{j}\omega\mu}{4\pi R}(Z_G + Z)^{-1} Z \times \begin{bmatrix} \mathbf{J_x} \\ \mathbf{J_y} \\ \mathbf{J_z} \\ -\mathbf{M_x} \\ -\mathbf{M_y} \\ -\mathbf{M_z} \end{bmatrix}^T \begin{bmatrix} (E_\theta\cos\theta\cos\phi - E_\phi\sin\phi)\mathbf{v}_i \\ (E_\theta\cos\theta\sin\phi + E_\phi\cos\phi)\mathbf{v}_i \\ -E_\theta\sin\theta\mathbf{v}_i \\ \frac{E_\theta\sin\phi + E_\phi\cos\theta\cos\phi}{\eta}\mathbf{v}_i \\ \frac{-E_\theta\cos\phi + E_\phi\cos\theta\sin\phi}{\eta}\mathbf{v}_i \\ \frac{-E_\phi\sin\theta}{\eta}\mathbf{v}_i \end{bmatrix} \quad (37)$$

where $\mathbf{v}_i = e^{\mathrm{j}(2\pi/\lambda)[\sin\theta(\mathbf{x}\cos\phi + \mathbf{y}\sin\phi) + \mathbf{z}\cos\theta]}$; Δs is the area of the discretizations assuming that they all have the same size; $\mathbf{J_x}$, $\mathbf{J_y}$, $\mathbf{J_z}$, $\mathbf{M_x}$, $\mathbf{M_y}$, and $\mathbf{M_z}$ are column vectors containing the electric and magnetic current x, y, and z components at discrete locations on the closed surface S; and the column vectors $\mathbf{x}$, $\mathbf{y}$, and $\mathbf{z}$ contain the x, y, and z coordinates of the discretizations. This can be extended in a straightforward manner to array antennas where multiple ports can be excited. In this case, E becomes a column vector instead of a scalar; the column vectors $\mathbf{J_x}$, $\mathbf{J_y}$, $\mathbf{J_z}$, $\mathbf{M_x}$, $\mathbf{M_y}$, and $\mathbf{M_z}$ become matrices with a number of columns equal to the number of ports; and Z_G and Z are the generator and impedance matrices defined in Section 2. This gives the following convenient expression:

$$\mathbf{E} = \tilde{C}_{tx}\mathbf{v}_{ideal} \quad (38)$$

where

$$\tilde{C}_{tx} = -\Delta s\frac{\mathrm{j}\omega\mu}{4\pi R}(Z_G + Z)^{-1} Z \begin{bmatrix} J_x \\ J_y \\ J_z \\ -M_x \\ -M_y \\ -M_z \end{bmatrix}^T \quad (39)$$

and

$$\mathbf{v}_{ideal} = \begin{bmatrix} \left(E_\theta\cos\theta\cos\phi - E_\phi\sin\phi\right)\mathbf{v}_i \\ (E_\theta\cos\theta\sin\phi + E_\phi\cos\phi)\mathbf{v}_i \\ -E_\theta\sin\theta\mathbf{v}_i \\ \frac{E_\theta\sin\phi + E_\phi\cos\theta\cos\phi}{\eta}\mathbf{v}_i \\ \frac{-E_\theta\cos\phi + E_\phi\cos\theta\sin\phi}{\eta}\mathbf{v}_i \\ \frac{-E_\phi\sin\theta}{\eta}\mathbf{v}_i \end{bmatrix}. \quad (40)$$

Table 1. Summary of the analytical formulations for evaluating mutual coupling in receive (Rx) and transmit (Tx) antenna systems [8].

Mode	Loading Conditions when Currents Determined	Impedance Form	Admittance Form
Rx	1) All elements loaded except excited one	$\tilde{C}_{rx} = -Z_L(Z_L + Z_{ANT})^{-1} Z_{ANT} I^T$	$\tilde{C}_{rx} = -(Y_L + Y_{ANT})^{-1} I^T$
	2) All elements loaded	$\tilde{C}_{rx} = -Z_L I_L^T$	$\tilde{C}_{rx} = -Y_L^{-1} I_L^T$
	3) All elements short-circuited	$\tilde{C}_{rx} = -Z_L(Z_L + Z)^{-1} Z I_{sc}^T$	$\tilde{C}_{rx} = -(Y_L + Y)^{-1} I_{sc}^T$
Tx	1) All elements loaded except excited one	$\tilde{C}_{tx} = -\frac{\mathrm{j}\omega\mu}{4\pi R}(Z_G + Z_{ANT})^{-1} Z_{ANT} I^T$	$\tilde{C}_{tx} = -\frac{\mathrm{j}\omega\mu}{4\pi R} Y_G (Y_G + Y_{ANT})^{-1} I^T$
	2) All elements loaded	$\tilde{C}_{tx} = -\frac{\mathrm{j}\omega\mu}{4\pi R} I_L^T$	$\tilde{C}_{tx} = -\frac{\mathrm{j}\omega\mu}{4\pi R} I_L^T$
	3) All elements short-circuited	$\tilde{C}_{tx} = -\frac{\mathrm{j}\omega\mu}{4\pi R}(Z_G + Z)^{-1} Z I_{sc}^T$	$\tilde{C}_{tx} = -\frac{\mathrm{j}\omega\mu}{4\pi R} Y_G (Y_G + Y)^{-1} I_{sc}^T$

Note: See the Appendix for details on the derivation of these analytical formulations.

The matrix $\tilde{C}_{tx}$ is independent of the direction of the observation and, as such, constitutes the coupling matrix estimate in a transmit antenna system. Unlike (13), this matrix has a nonsquare structure in general to characterize radiation for antennas of arbitrary geometry and composition. We note that the procedure for estimating the coupling matrix of a transmit system is similar to the five-step procedure of a receive system, described in Section 3.1, with the exception of the use of (39) instead of (20).

3.3 Formulation Variants and Reciprocity Relationships

Comparing the generalized analytical formulations of the receive and transmit systems, important similarities are observed. First, the ideal signal vectors of (26) and (40) are identical. Second, both coupling matrix estimates in (20) and (39) include the following common term:

$$I_{sc} = \Delta s \begin{bmatrix} J_x \\ J_y \\ J_z \\ -M_x \\ -M_y \\ -M_z \end{bmatrix}. \tag{41}$$

Although matrices J_x, J_y, J_z, M_x, M_y, and M_z were determined with all ports short-circuited in Sections 3.1 and 3.2, other formulations can be obtained for different loading conditions [8]. Restricting ourselves to the cases where voltage sources are used as excitations, let us define the three current matrices I, I_L, and I_{sc} for electric and magnetic currents determined *in transmit-mode* with 1) all elements loaded except the excited one, 2) all elements loaded, and 3) all elements short-circuited, respectively. The various derivations for evaluating the coupling matrix in receive and transmit antenna systems are presented in the Appendix, and the results are summarized in Table 1. The formulations can be expressed using either impedances or admittances, and the two different forms are thus given in the table. In case 1 with only the unexcited elements loaded, the diagonal matrices Z_{ANT} and Y_{ANT} are introduced. Their diagonal entries are simply the input impedances and admittances of the array elements. Case 1 corresponds to the approach employed in [9] and [89], where the current distribution and input impedance of each element are computed through the separate excitation of the element by a unit-voltage source, whereas all the other elements are terminated with the load impedances of the receivers. The input impedance of an element is then given by the inverse of the input current when this element is excited. It is important to note that the voltage source is directly applied at the excited port without any load. For a single antenna or for an array in the absence of mutual coupling, $Z_{ANT} = Z$, and $Y_{ANT} = Y$; otherwise, $Z_{ANT} \neq Z$, and $Y_{ANT} \neq Y$. The three different formulation cases have their advantages. Since the matrices Z_L and Z_{ANT} are both diagonal matrices, the first two formulation cases allow the estimation of complete rows of coupling matrices without having to excite all of the elements. This may be useful in complex antenna systems where only the performance of a subset of the system must be evaluated. The third formulation case does not have this feature due to the off-diagonal entries of matrix Z but is valid for arbitrary loads, unlike the two first cases. This may be useful for optimization purposes since the current distributions do not have to be recomputed for various loads. It also gives a very general relationship between receive and transmit formulations, i.e.,

$$\tilde{C}_{tx} = \frac{\mathrm{j}\omega\mu}{4\pi R}(Z_G + Z)^{-1}(Z_L + Z) Z_L^{-1} \tilde{C}_{rx}. \tag{42}$$

If $Z_L = Z_G$, (42) reduces to

$$\tilde{C}_{tx} = \frac{\mathrm{j}\omega\mu}{4\pi R} Z_L^{-1} \tilde{C}_{rx}. \tag{43}$$

The matrix Z_L in (43) is a diagonal matrix whose diagonal entries are the values of load impedances at the system ports. If all of these have equal values, we note the following relation between the two formulations:

$$\tilde{C}_{tx} = \frac{\mathrm{j}\omega\mu}{4\pi R Z_1} \tilde{C}_{rx} \tag{44}$$

where Z_1 is the common load impedance value. Since $j\omega\mu/4\pi RZ_1$ is simply a complex scaling factor, it is seen that

$$\tilde{C}_{tx} \propto \tilde{C}_{rx}. \tag{45}$$

This has important consequences because it implies that *transmit and receive formulations can be used interchangeably for compensating mutual coupling when the load and generator impedances are all equal*. In general, only the relative amplitudes and phases are required, and therefore, the scaling factor has little importance in the compensation. For systems where the load impedances are not equal, a correction must be made before interchanging the two formulations. The latter is embodied in the following equation:

$$\tilde{C}_{tx} \propto Z_L^{-1}\tilde{C}_{rx}. \tag{46}$$

This important relationship can be very useful in the compensation of transmit arrays and in retrodirective systems. The theory presented here will be used in Section 5 in these two applications.

4. Efficiency of Mutual Coupling Compensation

The analytical formulations in Table 1 generally give matrices that have a number of rows equal to the number of array elements and a number of columns governed by the discretizations of closed surfaces. Hence, in general, we are dealing with nonsquare matrices that have significantly more columns than rows. However, it is possible to reduce the number of columns through careful consideration of the system physics [89].

The case of a system consisting entirely of a perfect electric conductor (PEC) is an interesting example. Since the closed surfaces of integration can be defined at the surfaces of PEC, the magnetic equivalent currents $\vec{M}_{eq}$ vanish by boundary conditions, and the sizes of the coupling matrix estimates $\tilde{C}_{rx}$ and $\tilde{C}_{tx}$ are reduced by half.

The case of thin-wire elements, such as monopoles or dipoles, is another interesting example. If the wires are vertically oriented and consist of a PEC, horizontal electric currents J_x and J_y and all magnetic currents vanish, leaving only the electric currents J_z in the evaluation of $\tilde{C}_{rx}$ and $\tilde{C}_{tx}$. Furthermore, if we are only interested in one elevation angle θ, the current matrix can be rearranged to (47),

$$I = \Delta s \begin{bmatrix} \sum_{k=1}^{K_1} J_{zk1} e^{j\frac{2\pi}{\lambda} z_k \cos\theta} & \cdots & \sum_{k=1}^{K_1} J_{zkN} e^{j\frac{2\pi}{\lambda} z_k \cos\theta} \\ \sum_{k=K_1+1}^{K_2} J_{zk1} e^{j\frac{2\pi}{\lambda} z_k \cos\theta} & \cdots & \sum_{k=K_1+1}^{K_2} J_{zkN} e^{j\frac{2\pi}{\lambda} z_k \cos\theta} \\ \vdots & \ddots & \vdots \\ \sum_{k=K_{N-1}+1}^{K_N} J_{zk1} e^{j\frac{2\pi}{\lambda} z_k \cos\theta} & \cdots & \sum_{k=K_{N-1}+1}^{K_N} J_{zkN} e^{j\frac{2\pi}{\lambda} z_k \cos\theta} \end{bmatrix} \tag{47}$$

where J_{zkn} is the entry of J_z at its kth row and nth column, z_k is the vertical location of the kth wire segment, and K_1 to K_N are the last segment numbers for elements 1 to N. The ideal signal vector then takes the following form:

$$\mathbf{v}_{ideal} = -E_\theta \sin\theta \begin{bmatrix} e^{j\frac{2\pi}{\lambda}\sin\theta(x_1\cos\phi + y_1\sin\phi)} \\ e^{j\frac{2\pi}{\lambda}\sin\theta(x_2\cos\phi + y_2\sin\phi)} \\ \vdots \\ e^{j\frac{2\pi}{\lambda}\sin\theta(x_N\cos\phi + y_N\sin\phi)} \end{bmatrix} \tag{48}$$

where x_n and y_n are the horizontal locations of the nth wire. Substituting (47) into the formulations in Table 1 gives square matrices $\tilde{C}_{rx}$ and $\tilde{C}_{tx}$. Further to the significant reduction in memory requirement for storing the coupling parameters, the matrix is invertible and can be used in (15) to estimate incident signals in a receive system. We note that this size reduction is consistent with [50–57] and [59–78], where a square structure is assumed for the coupling matrix.

Unfortunately, for other systems, the number of coupling parameters may become huge. For this reason, it is desirable to study approaches that can reduce this number while maintaining acceptable mutual coupling compensation accuracy. As discussed in [89], the calibration method in [59–61] can be extended to handle antenna systems of arbitrary geometries. This is done by judiciously appending rows to the ideal signal vectors prior to mapping them to the measured vectors. These additional rows must account for the response to signals of various polarizations at locations distributed over the whole structure of the antenna system. Acceptable accuracy can be obtained for electrical spacings on this structure that are significantly larger than those required for the computation of current distributions. The ideal signal vectors then take the same form as (26) and (40) but with reduced dimensions. Through careful consideration of the system physics, it is possible to reduce the dimensions even more in a similar fashion as previously described based on the materials, geometry, and the absence of response to some polarizations. Steering vectors must be recorded for M discrete directions/polarizations in the following matrix:

$$V = [\mathbf{v}_{rx_1} \quad \mathbf{v}_{rx_2} \quad \cdots \quad \mathbf{v}_{rx_M}] \tag{49}$$

and the ideal signal vectors associated with these measured vectors are recorded in

$$V_{ideal} = [\mathbf{v}_{ideal_1} \quad \mathbf{v}_{ideal_2} \quad \cdots \quad \mathbf{v}_{ideal_M}]. \tag{50}$$

The coupling matrix is then estimated through a least squares approximation of $\tilde{C}$ in $V = \tilde{C}V_{ideal}$ using

$$\tilde{C} = VV_{ideal}{}^H\left(V_{ideal}V_{ideal}{}^H\right)^{-1} \tag{51}$$

where $(\cdot)^H$ denotes the conjugate transpose operation. The condition for solution uniqueness is that the number of measurements be at least equal to the number of rows of V_{ideal}. This approach was demonstrated to be superior to any

existing interpolation technique in [90] for both simple and complex geometries.

The accuracy of $\tilde{C}$ is highly dependent on the structure of V_{ideal} and the number of calibration points M specified by the engineer. As discussed in [89–91], the condition number of $V_{ideal}V_{ideal}^{H}$ can be closely monitored as an indication of the best number of columns for $\tilde{C}$. If the matrix $\tilde{C}_{rx}$ is available, M can be arbitrarily increased, and a hybrid approach can be devised to benefit from both a large number of steering vectors and a reduced number of coupling parameters. This hybrid approach estimates a smaller coupling matrix than $\tilde{C}_{rx}$ through a least squares approximation of $\tilde{C}$ in $V = \tilde{C}_{rx}V_{ideal}{}' = \tilde{C}V_{ideal}$ using

$$\tilde{C} = \tilde{C}_{rx}V_{ideal}{}'V_{ideal}{}^{H}\left(V_{ideal}V_{ideal}{}^{H}\right)^{-1} \tag{52}$$

where $V_{ideal}{}'$ contains the ideal signal vectors whose dimensions are consistent with $\tilde{C}_{rx}$. The reader is referred to [89] for more details on this methodology.

5. Applications

5.1 Retrodirective Systems

The reciprocity relationships derived in Section 3 can be used to explain and extend the theory of retrodirective arrays. These arrays operate in such a way that incident signals are retransmitted in the same directions that they are received without sophisticated signal processing equipment in the front-end. Although various techniques are available for achieving retrodirectivity, the most popular is the Pon array [92], which exploits the heterodyne technique where a frequency mixer is connected at each of the array elements to perform phase conjugation of the received signals. Using the Schwarz inequality, [93] and [94] proved that this phase conjugation gives optimal performance even in the presence of strong mutual coupling. The theory presented in Section 3 certainly supports this conclusion. However, to consider the case of nonuniform loads, the conventional circuit model of Pon arrays can be extended to that in Figure 2, where the signals at the elements are scaled by the inverse of the conjugated load impedances.

5.1.1 Polarization Diverse Systems

The theory in Section 3 can be verified in a straightforward fashion using proven electromagnetic codes. More specifically, the numerical electromagnetic code (NEC) [95], which is a method of moments solver, is used here to model a circular array consisting of four crossed dipole pairs shown in Figure 3. Each of the pairs is comprised of two orthogonal half-wave dipoles centrally terminated into individual load impedances of 50 Ω. The array radius is equal to $\lambda/4$. Circular arrays are a popular choice due to their compactness and the absence of ambiguities in azimuth. The horizontal dipoles

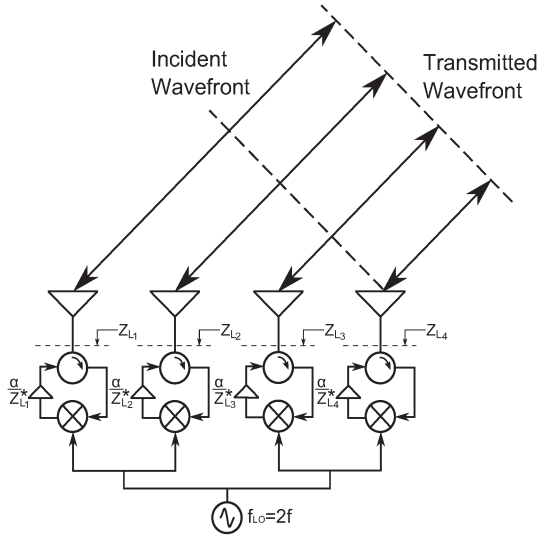

Figure 2. Compensated circuit model of a Pon retrodirective array consisting of four elements. Received signals at frequency f are passed through circulators and are mixed with a local oscillator whose frequency is $2f$. The signal components at frequency f at the output of the mixers are complex conjugates of the input signals. These signals are then amplified before being returned to the antennas through the circulators. Amplification is scaled by $1/Z_{L_n}{}^*$ to take into consideration nonuniform loading.

add sensitivity to horizontally polarized signals. Since the horizontal and vertical dipoles are individually terminated, the system provides polarization agility and can handle signals of arbitrary polarizations. This kind of array is therefore very useful for verifying the theory presented in this paper, which has been generalized for arbitrary polarizations.

Two approaches are available for verifying the theory. The first approach is more straightforward and involves the excitation of the numerical model in receive-mode by an incident plane wave. The complex conjugates of the received voltages are then used as the values of voltage sources in transmission, and the resulting radiated electromagnetic fields are computed. If the theory is correct, radiation should be maximized in the direction of the incident plane wave

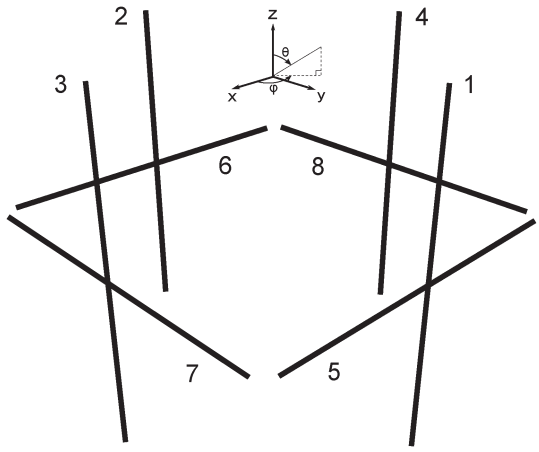

Figure 3. Circular array of four crossed dipole pairs.

assuming an active implementation of the retrodirective system where scattered fields can be ignored. The second approach avoids a simulation in the receive-mode and computes the coupling matrix of the system using the theory applicable to receive systems in Section 3. This approach is favored here since it will be reused in Section 5.2. Using the equations in Table 1, the current matrix required in the computation of the coupling matrix estimate takes the following form:

$$I = \Delta \begin{bmatrix} [I_z] \\ [I_x] \\ [I_y] \end{bmatrix} = \Delta \begin{bmatrix} \begin{bmatrix} \mathbf{I}_{11} & \mathbf{I}_{12} & \cdots & \mathbf{I}_{18} \\ \mathbf{I}_{21} & \mathbf{I}_{22} & \cdots & \mathbf{I}_{28} \\ \mathbf{I}_{31} & \mathbf{I}_{32} & \cdots & \mathbf{I}_{38} \\ \mathbf{I}_{41} & \mathbf{I}_{42} & \cdots & \mathbf{I}_{48} \end{bmatrix} \\ \begin{bmatrix} \mathbf{I}_{51} & \mathbf{I}_{52} & \cdots & \mathbf{I}_{58} \\ \mathbf{I}_{61} & \mathbf{I}_{62} & \cdots & \mathbf{I}_{68} \end{bmatrix} \\ \begin{bmatrix} \mathbf{I}_{71} & \mathbf{I}_{72} & \cdots & \mathbf{I}_{78} \\ \mathbf{I}_{81} & \mathbf{I}_{82} & \cdots & \mathbf{I}_{88} \end{bmatrix} \end{bmatrix} \tag{53}$$

where Δ is the segment length of the discretized dipoles, and the column vectors $\mathbf{I}_{ij}$ contain the electric current distributions on dipole i due to the excitation of dipole j. The dipoles are modeled with thin wires; hence, currents are used in (53) as opposed to current densities in (20), and the segment length Δ is used instead of the segment area Δs. The wires are assumed to be made of a PEC, and all magnetic currents are thus ignored. This formulation assumes that the first four dipoles are vertical; hence, only z-directed currents are considered for these dipoles using submatrix $[I_z]$. The fifth and sixth dipoles are horizontal and oriented along the x-axis; hence, only x-directed currents are considered for these two dipoles using submatrix $[I_x]$. The seventh and eighth dipoles are horizontal and oriented along the y-axis; hence, only y-directed currents are considered for these two dipoles using submatrix $[I_y]$. The ideal vector containing the incident signals takes the following form:

$$\begin{aligned} &\mathbf{v}_{ideal}(\phi, \theta, E_\theta, E_\phi) \\ &= \begin{bmatrix} -E_\theta \sin\theta \begin{bmatrix} e^{\mathrm{j}\frac{2\pi}{\lambda}\left(\frac{\lambda}{4}\sin\theta\sin\phi + \mathbf{z}_1\cos\theta\right)} \\ e^{\mathrm{j}\frac{2\pi}{\lambda}\left(-\frac{\lambda}{4}\sin\theta\sin\phi + \mathbf{z}_2\cos\theta\right)} \\ e^{\mathrm{j}\frac{2\pi}{\lambda}\left(\frac{\lambda}{4}\sin\theta\cos\phi + \mathbf{z}_3\cos\theta\right)} \\ e^{\mathrm{j}\frac{2\pi}{\lambda}\left(-\frac{\lambda}{4}\sin\theta\cos\phi + \mathbf{z}_4\cos\theta\right)} \end{bmatrix} \\ (E_\theta\cos\theta\cos\phi - E_\phi\sin\phi) \begin{bmatrix} e^{\mathrm{j}\frac{2\pi}{\lambda}\sin\theta\left(\mathbf{x}_5\cos\phi + \frac{\lambda}{4}\sin\phi\right)} \\ e^{\mathrm{j}\frac{2\pi}{\lambda}\sin\theta\left(\mathbf{x}_6\cos\phi - \frac{\lambda}{4}\sin\phi\right)} \end{bmatrix} \\ (E_\theta\cos\theta\sin\phi + E_\phi\cos\phi) \begin{bmatrix} e^{\mathrm{j}\frac{2\pi}{\lambda}\sin\theta\left(\frac{\lambda}{4}\cos\phi + \mathbf{y}_7\sin\phi\right)} \\ e^{\mathrm{j}\frac{2\pi}{\lambda}\sin\theta\left(-\frac{\lambda}{4}\cos\phi + \mathbf{y}_8\sin\phi\right)} \end{bmatrix} \end{bmatrix} \end{aligned} \tag{54}$$

where the column vectors $\mathbf{x}_n$, $\mathbf{y}_n$, and $\mathbf{z}_n$ contain the physical locations of the segments of the nth dipole. It is implicitly assumed in this formulation that the vertical and horizontal dipoles are centered at $(x_1, y_1, z_1) = (x_5, y_5, z_5) = (0, \lambda/4, 0)$, $(x_2, y_2, z_2) = (x_6, y_6, z_6) = (0, -(\lambda/4), 0)$, $(x_3, y_3, z_3) = (x_7, y_7, z_7) = (\lambda/4, 0, 0)$, and $(x_4, y_4, z_4) = (x_8, y_8, z_8) = (-(\lambda/4), 0, 0)$, respectively.

The dipoles were discretized using 11 segments per dipole; hence, the coupling matrix estimate in reception $\tilde{C}_{rx}$ is an 8×88 matrix. The computation by NEC required approximately 65 kB of storage and 0.1 s of runtime to obtain each column of (53). The received voltages can be estimated for an arbitrary illumination using

$$\mathbf{v}_{rx}(\phi, \theta, E_\theta, E_\phi) = \tilde{C}_{rx}\mathbf{v}_{ideal}(\phi, \theta, E_\theta, E_\phi) \tag{55}$$

which requires 704 complex operations. Since the array is uniformly loaded, the complex conjugate of (55) can be used directly as the excitation of a transmit system of identical geometry and whose generator impedances are equal to the 50-Ω loads, according to the following equation:

$$\mathbf{v}_{tx} = \mathbf{v}_{rx}(\phi, \theta, E_\theta, E_\phi)^* \tag{56}$$

where $(\cdot)^*$ denotes the complex conjugate operation. To confirm that this is correct, (55) is used to estimate the received voltages for a vertically polarized signal arriving from azimuth angles $\phi = 0°$, $30°$, $60°$, and $90°$ for elevation angles $\theta = 90°$ and $45°$. This is done by computing $\mathbf{v}_{ideal}(0°, 90°, 1, 0)$, $\mathbf{v}_{ideal}(30°, 90°, 1, 0)$, $\mathbf{v}_{ideal}(60°, 90°, 1, 0)$, $\mathbf{v}_{ideal}(90°, 90°, 1, 0)$, $\mathbf{v}_{ideal}(0°, 45°, 1, 0)$, $\mathbf{v}_{ideal}(30°, 45°, 1, 0)$, $\mathbf{v}_{ideal}(60°, 45°, 1, 0)$, and $\mathbf{v}_{ideal}(90°, 45°, 1, 0)$ using (54) and substituting this into (55). These results are then substituted into (56) and used directly in a numerical simulation in transmission. Voltage sources having the values contained in $\mathbf{v}_{tx}$ are applied at the element ports, while including generator impedances $Z_G = 50\ \Omega$, and the θ-component of the radiated electric fields are calculated using NEC. Note that the horizontal dipoles do not contribute to radiation for $\theta = 90°$ due to the vertical polarization of the incident signal, but they do for $\theta = 45°$ because a horizontal incident field exists for vertically polarized signals arriving from $\theta \neq 90°$. The results are shown in Figure 4. For comparison, the results of a Van Atta implementation are also presented [96]. In this case, phase conjugation is attempted using $\mathbf{v}_{tx} = [v_{rx_2} v_{rx_1} v_{rx_4} v_{rx_3} v_{rx_6} v_{rx_5} v_{rx_8} v_{rx_7}]^T$. It is seen in Figure 4 that the use of (56) gives very satisfying performance in all the plotted scenarios since the transmitted power is maximized in the directions of the incident signals. By comparing the radiation patterns for $\phi = 0°$ and $\phi = 90°$, it is verified that the radiation patterns repeat in each quadrant due to the symmetry of the system. As discussed in [97] and [98], the performance of the Van Atta implementation is seen to be suboptimal due to mutual coupling effects with reduced power levels in the directions of incident signals.

5.1.2 Nonuniformly Loaded Systems

To evaluate the impact of ignoring nonuniform loading, the linear array shown in Figure 5 is now considered. This array consists of dipoles having lengths decreasing from 0.6λ to 0.3λ as we move along the x-axis and whose loads are the complex conjugate of their self-impedances. The coupling matrix can be estimated using the current matrix given by

$$I = \Delta I_z = \Delta \begin{bmatrix} \mathbf{I}_{11} & \mathbf{I}_{12} & \cdots & \mathbf{I}_{17} \\ \mathbf{I}_{21} & \mathbf{I}_{22} & \cdots & \mathbf{I}_{27} \\ \vdots & \vdots & \ddots & \vdots \\ \mathbf{I}_{71} & \mathbf{I}_{72} & \cdots & \mathbf{I}_{77} \end{bmatrix}. \tag{57}$$

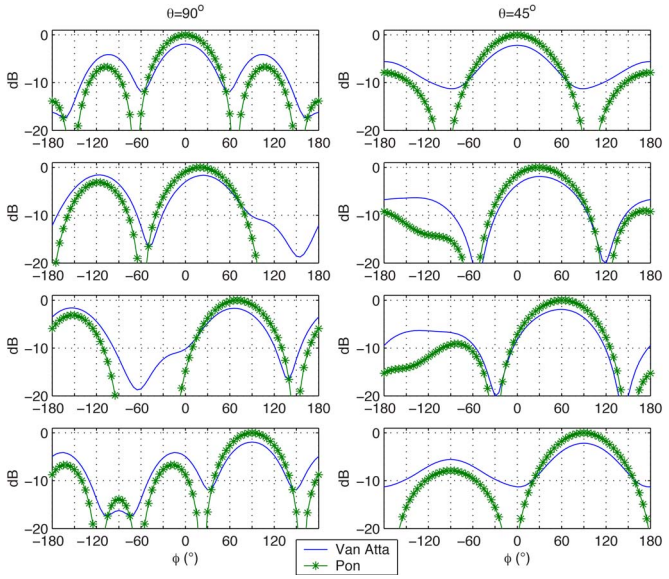

Figure 4. Retrodirective radiation patterns of the circular array of four crossed dipole pairs in Figure 3 illuminated by a vertically polarized signal arriving from $\phi = 0°$, $\phi = 30°$, $\phi = 60°$, and $\phi = 90°$, respectively (top to bottom plots). The radiation patterns on the left are for an elevation angle of 90°, and those on the right are for an elevation angle of 45°. The Pon implementation is seen to give better results than the Van Atta due to mutual coupling effects, with optimized radiation and a main beam in the direction of the incident signal.

The currents in (57) were computed using NEC, which required approximately 54 kB of storage and less than 0.1 s of runtime to obtain each column of matrix I with each of the elements discretized into 11 segments. Noting that the array elements only respond to vertically polarized signals, the parameters E_θ and E_ϕ can be ignored, and the ideal signal vector is given by

$$\mathbf{v}_{ideal}(\phi,\theta) = -\sin\theta \begin{bmatrix} e^{j\frac{2\pi}{\lambda}(0.3\lambda \sin\theta\cos\phi + \mathbf{z}_1\cos\theta)} \\ e^{j\frac{2\pi}{\lambda}(0.6\lambda \sin\theta\cos\phi + \mathbf{z}_2\cos\theta)} \\ \vdots \\ e^{j\frac{2\pi}{\lambda}(2.1\lambda \sin\theta\cos\phi + \mathbf{z}_7\cos\theta)} \end{bmatrix}. \quad (58)$$

For a similar system used in transmission and having generator impedances given by $Z_G = Z_L$, the values of the voltage sources are determined using

$$\mathbf{v}_{tx} = \left[Z_L{}^{-1}\mathbf{v}_{rx}(\phi,\theta)\right]^* = \left[Z_L{}^{-1}\tilde{C}_{rx}\mathbf{v}_{ideal}(\phi,\theta)\right]^*. \quad (59)$$

The θ-component of the radiated electric field of the transmit system is plotted in Figure 6 for an incident signal arriving from azimuth angles $\phi = 0°$, 60°, 120°, and 180° for elevation angles $\theta = 90°$ and 45°. For comparison, the results are also shown when the nonuniform loading is ignored. This is equivalent to simply assuming that Z_L is proportional to the identity matrix in (59). It is observed here that the consideration of nonuniform loading is critical

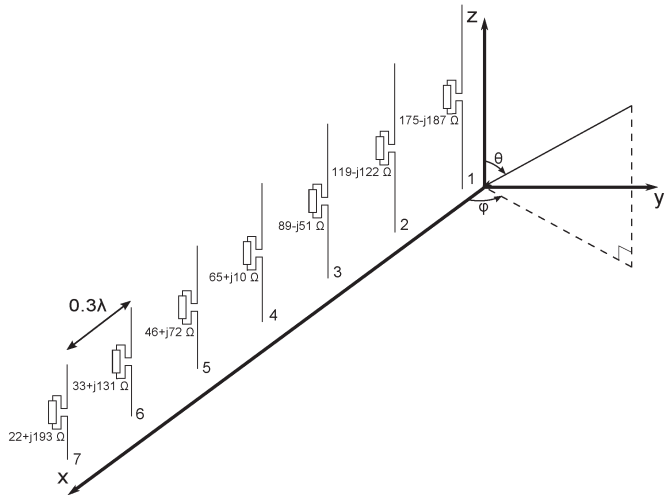

Figure 5. Nonuniform linear array of seven nonuniformly loaded vertical dipoles. Each dipole has a different length and is terminated with a load impedance equal to the complex conjugate of its self-impedance.

in the implementation of retrodirective systems; otherwise, suboptimal performance is possible. All the retrodirective patterns obtained with proper consideration of nonuniform loading are verified to be satisfactory with their main beams pointing in the directions of the incident signal. These results strongly support the theory in Section 3 and the circuit model in Figure 2.

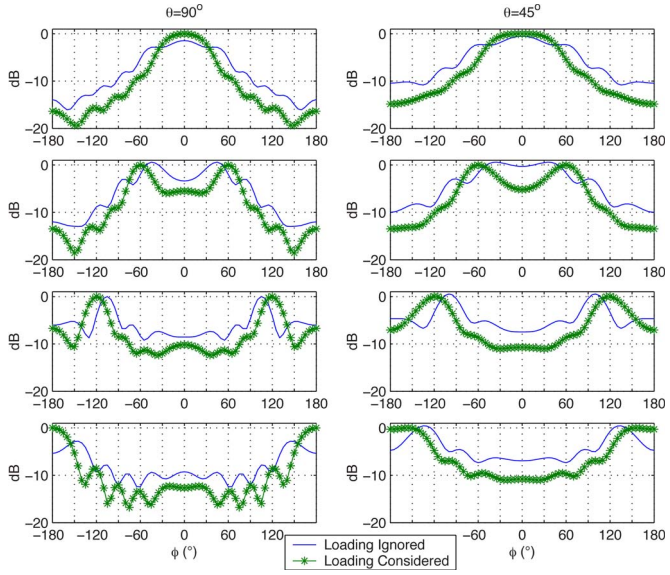

Figure 6. Retrodirective radiation patterns of the nonuniform linear array of seven vertical dipoles in Figure 5 illuminated by a vertically polarized signal arriving from $\phi = 0°$, $\phi = 60°$, $\phi = 120°$, and $\phi = 180°$, respectively (top to bottom plots). The radiation patterns on the left are for an elevation angle of 90°, and those on the right are for an elevation angle of 45°. It is seen that the nonuniform loads must be carefully considered to obtain optimized radiation with a main beam directed toward the incident signal.

5.2 Receive/Transmit Beamforming

Beamforming is a popular application in receive antenna systems for maximizing the reception of a desired signal while minimizing interference. To perform beamforming in transmission, the directions and polarizations of distant receive systems must be known. The reciprocity relationships in Section 3 give us the confidence to use received quantities for transmission. This is studied in this section where transmit systems are calibrated using coupling matrices and signals processed in reception.

5.2.1 Polarization Diverse Systems

The circular array of four crossed dipole pairs illustrated in Figure 3 is first considered. In accordance with the theory in Section 3, since all the elements are terminated in equal loads, the receive coupling matrix estimate $\tilde{C}_{rx}$, derived in Section 5.1, can also be used here to compensate mutual coupling in transmission. Unlike the retrodirective system in Section 5.1 where coupling matrices were only employed for analysis purposes, the reduction of the matrix size is desirable in a transmit beamformer to minimize the memory requirement and computations in a practical implementation. Using the hybrid approach introduced in Section 4, the size of the matrix is further reduced to 8×40, for a total of 320 stored complex coupling parameters instead of 704. This is done by subdividing each of the eight dipoles into five larger segments instead of the 11 used in the numerical evaluation of $\tilde{C}_{rx}$. The column vectors $\mathbf{x}_n$, $\mathbf{y}_n$, and $\mathbf{z}_n$ in the ideal signal vector of (54) therefore consist of five entries.

Using the 8×40 matrix $\tilde{C}$ obtained by (52), a correlation matrix assuming six uncorrelated signals is generated using

$$R_{xx} = \tilde{C}\left[\sum_{i=1}^{6} \mathbf{v}_{ideal}\left(\phi_i, \theta_i, E_{\theta_i}, E_{\phi_i}\right) \times \mathbf{v}_{ideal}\left(\phi_i, \theta_i, E_{\theta_i}, E_{\phi_i}\right)^H\right]\tilde{C}^H + \sigma_o^2 I_N \quad (60)$$

where $(\cdot)^H$ is the conjugate transpose operation; ϕ_i, θ_i, E_{θ_i}, and E_{ϕ_i} are the arrival and polarization parameters describing the ith signal; I_N is the identity matrix whose dimensions are equal to the number of array elements $N = 8$; and $\sigma_o^2 = 0.00001$ is a fictitious noise power used for loading the diagonal of R_{xx} to ensure a reasonable condition number. The noise is hereby modeled as uncorrelated zero-mean additive white Gaussian. This example considers a scenario involving six signals at an elevation of $\theta = 45°$. Two of these are right-hand circularly polarized (RHCP) signals arriving from $\phi = 0°$ and $60°$, two are left-hand circularly polarized (LHCP) signals arriving from $\phi = -30°$ and $30°$, one is a horizontally polarized signal arriving from $\phi = -90°$, and one is a vertically polarized signal arriving from $\phi = -120°$. Radiation is optimized in the direction of the vertically polarized signal at $\phi = -120°$, and all other signals are considered as interferers. The voltage sources of this system in transmission are then determined using

$$\mathbf{v}_{tx} = \left[R_{xx}^{-1}\tilde{C}\mathbf{v}_{ideal}(-120°, 45°, 1, 0)\right]^*. \quad (61)$$

Using these voltage sources in the numerical model in transmission, the radiated electric field components $E_\theta(\phi, \theta)$ and $E_\phi(\phi, \theta)$ are computed with NEC. The radiation patterns in transmission at an elevation of $\theta = 45°$ for the four different polarizations of the signals are plotted in Figure 7. These patterns are obtained through the following combinations of the two orthogonal field components:

$$\begin{aligned} E_v(\phi, \theta) &= E_\theta(\phi, \theta) \\ E_h(\phi, \theta) &= E_\phi(\phi, \theta) \\ E_{RHCP}(\phi, \theta) &= jE_\theta(\phi, \theta) + E_\phi(\phi, \theta) \\ E_{LHCP}(\phi, \theta) &= E_\theta(\phi, \theta) + jE_\phi(\phi, \theta) \end{aligned} \quad (62)$$

where the subscripts v, h, $RHCP$, and $LHCP$ stand for vertical, horizontal, right-hand circular, and left-hand circular polarizations, respectively.

The results in Figure 7 are very satisfying since nulls are formed in transmission not only in the directions of the five interferers but also with the correct polarizations and, thus, confirm that coupling matrices are effective in mutual coupling compensation of both receive and transmit

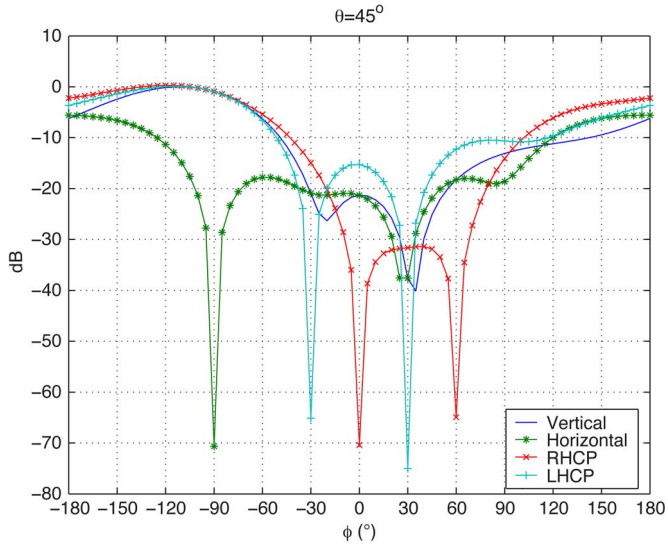

Figure 7. Radiation patterns in transmission of the circular array of four crossed dipole pairs in Figure 3 for receivers of various polarizations at an elevation of 45° using an 8 × 40 coupling matrix estimate. Radiation is maximized for a vertically polarized receiver at −120° and minimized for a horizontally polarized receiver at −90°, LHCP receivers at −30° and 30°, and RHCP receivers at 0° and 60°. Mutual coupling is compensated effectively with a main beam and deep nulls forming in these directions.

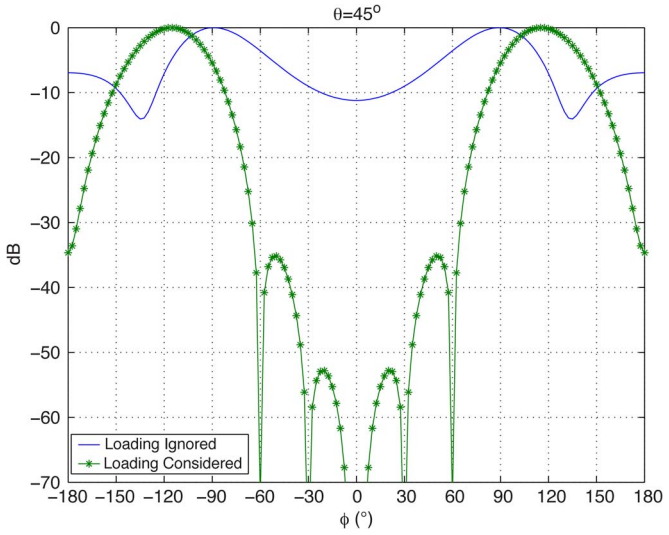

Figure 8. Radiation patterns in transmission of the nonuniform linear array of seven vertical dipoles in Figure 5 for receivers at an elevation of 45° using a 7 × 35 coupling matrix estimate. Radiation needs to be maximized at −120° and minimized at −60°, −30°, 0°, 30°, and 60°. It is seen that the nonuniform loads must be carefully considered to obtain optimized radiation with properly directed main beam and deep nulls.

beamforming systems. By reciprocity, it is expected that antennas both transmit and receive with the same polarizations. These results suggest that a wireless network can be optimized when signals are transmitted and received using the same antennas, and proper mutual coupling compensation is implemented. Note that if the desired signal waveform is known and all signals are being transmitted by distant systems, $\mathbf{v}_{tx}$ in (61) can also be determined through adaptive techniques without knowledge of $\tilde{C}$ and the desired signal's direction and polarization. The theory presented in this paper confirms that both deterministic and adaptive approaches can be effective in the optimization of wireless networks.

5.2.2 Nonuniformly Loaded Systems

The nonuniform linear array of seven dipoles shown in Figure 5 is now considered to study the impact of nonuniform loading in beamforming. The coupling matrix of this system in reception $\tilde{C}_{rx}$, derived in Section 5.1, is reduced using the hybrid approach in Section 4 to a 7 × 35 $\tilde{C}$ matrix, for a total of 245 stored complex coupling parameters instead of 539. Although the dipoles are of different lengths, a reduced discretization scheme involving five segments per dipole is nonetheless used in this example. The column vector $\mathbf{z}_n$ in the ideal signal vector of (58) therefore contains five entries instead of the 11 entries used with the original matrix.

Using the 7 × 35 matrix $\tilde{C}$ obtained by (52) and the same six-signal scenario as in Section 5.2.1, the correlation matrix estimated in reception, i.e., R_{xx}, can be used to determine the required voltage sources in transmission. However, nonuniform loading must be accounted for as follows:

$$\begin{aligned}\mathbf{v}_{tx} &= \left\{\left[Z_L^{-1}R_{xx}\left(Z_L^{H}\right)^{-1}\right]^{-1}Z_L^{-1}\tilde{C}\mathbf{v}_{ideal}(-120^\circ,45^\circ)\right\}^{*}\\ &= \left[Z_L^{H}R_{xx}^{-1}\tilde{C}\mathbf{v}_{ideal}(-120^\circ,45^\circ)\right]^{*}\end{aligned} \tag{63}$$

where the parameters E_θ and E_ϕ are ignored due to the pure vertical polarization of the antenna system. The resulting radiation patterns in transmission are presented in Figure 8 along with those obtained when nonuniform loading is ignored. It is seen that optimum beamforming is achieved since the main beam is in the direction of the desired signal while deep nulls form in the directions of the interferers. As already observed in Section 5.1, the main beam of the radiation pattern is adversely affected when nonuniform loading is ignored in a system where load impedances significantly vary. It is seen that interference nulling would also significantly suffer by the improper compensation of this transmit system, with attenuation of no more than 12 dB in the directions of the interferers.

5.3 DOA/Polarization Estimation

In some applications, it is necessary to estimate the DOA and polarization of incident signals. Accurate mutual coupling compensation is critical in such applications since it directly affects the accuracy and resolution of the estimator. The eight-dipole array in front of a rectangular conducting plate, similar to that in [80], is considered here. This antenna system is illustrated in Figure 9. For 2-D operation, the coupling matrix is estimated as indicated in the figure. The left part of the matrix is associated with the dipoles and uses row vectors $\mathbf{c}_{ij}$, whereas the rectangular conducting plate is subdivided along the horizontal and vertical axes to account for the variable horizontal and vertical phase shifts of incident

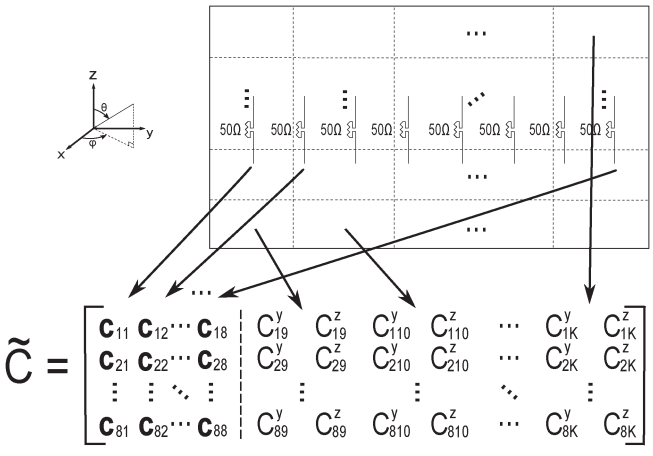

Figure 9. Geometry of the eight-dipole array in front of a conducting plate for 2-D operation. Eight row vectors associated with the dipoles fill the left part of the coupling matrix for each of its rows, whereas the other columns are associated with the different portions of the plate.

signals. Due to the finite dimensions of the conducting plate, the polarizations of the array elements may have horizontal components, and both horizontally and vertically oriented incident fields have to be accounted for on the plate using the complex scalar parameters C_{ij}^{y} and C_{ij}^{z}, respectively.

This antenna system is modeled with FEKO [99] using the method of moments. The dipoles are modeled by thin wires having a length of 6.12 cm, spaced 4.9 cm apart, and centrally terminated into 50-Ω load impedances. The rectangular plate is modeled by a thin 39.16-cm-wide and 24-cm-high perfectly conducting surface, located 3 cm behind the dipoles. The numerical calculations are performed for an operating frequency of 2.45 GHz. Reordering the entries of the right part of the matrix for mathematical conciseness, the coupling matrix estimate is obtained by the equations in Table 1 with the current matrix having the following form:

$$I=\begin{bmatrix}\Delta z[I_{wires}]\\ \Delta s\begin{bmatrix}J_z\\ J_y\end{bmatrix}\end{bmatrix}=\begin{bmatrix}\Delta z\begin{bmatrix}\mathbf{I}_{11} & \cdots & \mathbf{I}_{18}\\ \vdots & \ddots & \vdots\\ \mathbf{I}_{81} & \cdots & \mathbf{I}_{88}\end{bmatrix}\\ \Delta s\begin{bmatrix}J_{z91} & \cdots & J_{z98}\\ \vdots & \ddots & \vdots\\ J_{zK1} & \cdots & J_{zK8}\\ J_{y91} & \cdots & J_{y98}\\ \vdots & \ddots & \vdots\\ J_{yK1} & \cdots & J_{yK8}\end{bmatrix}\end{bmatrix} \tag{64}$$

where Δz and Δs are the dipole segment length and conducting plate patch area, respectively, $\mathbf{I}_{ij}$ is a column vector containing the electric currents on the segments of element i due to the excitation of element j, and J_{yij} and J_{zij} are the y- and z-directed electric current densities on patch i of the conducting plate due to the excitation of element j. The ideal signal vector of this problem takes the following form:

$$\mathbf{v}_{ideal}(\phi,\theta,E_\theta,E_\phi)=\begin{bmatrix}-E_\theta\sin\theta\begin{bmatrix}e^{j\frac{2\pi}{\lambda}[\sin\theta(\mathbf{x}_1\cos\phi+\mathbf{y}_1\sin\phi)+\mathbf{z}_1\cos\theta]}\\ \vdots\\ e^{j\frac{2\pi}{\lambda}[\sin\theta(\mathbf{x}_8\cos\phi+\mathbf{y}_8\sin\phi)+\mathbf{z}_8\cos\theta]}\\ e^{j\frac{2\pi}{\lambda}(y_9\sin\theta\sin\phi+z_9\cos\theta)}\\ \vdots\\ e^{j\frac{2\pi}{\lambda}(y_K\sin\theta\sin\phi+z_K\cos\theta)}\end{bmatrix}\\ (E_\theta\cos\theta\sin\phi+E_\phi\cos\phi)\begin{bmatrix}e^{j\frac{2\pi}{\lambda}(y_9\sin\theta\sin\phi+z_9\cos\theta)}\\ \vdots\\ e^{j\frac{2\pi}{\lambda}(y_K\sin\theta\sin\phi+z_K\cos\theta)}\end{bmatrix}\end{bmatrix} \tag{65}$$

where $\mathbf{x}_j$, $\mathbf{y}_j$, and $\mathbf{z}_j$ are column vectors containing the x, y, and z physical locations of the wire segments for $j \leq 8$, and y_j and z_j are scalar values of the y and z locations of the conducting plate patches for $j \geq 9$. Note that this formulation assumes that the conducting plate is located at $x = 0$. The numerical solution of this problem involved a total of 104 wire segments and 2923 surface patches, which required approximately 150 MB of storage and 51 s of runtime to obtain each of the columns of (64). Since two columns are required to account for both y- and z-directed currents on each patch, the coupling matrix estimate turns out to be an 8×5950 matrix. Using the size-reduction guidelines presented in Section 4, the size of the estimate can be reduced at the expense of some performance degradation. Here, the method is implemented by subdividing the wires into five segments, each for a total of 40 wire segments instead of 104, and the conducting plate into 70 patches, 10 wide by 7 high, instead of 2923. The size of the coupling matrix estimate then reduces to 8×180, for a total of 1440 stored complex coupling parameters instead of 47 600. This is done by computing the steering vectors for both vertically and horizontally polarized signals arriving from $-85 \leq \phi \leq 85°$ and $2.5 \leq \theta \leq 172.5°$ with angular increments of 10°. These two sets of steering vectors are obtained by substituting $\mathbf{v}_{ideal}(\phi,\theta,1,0)$ and $\mathbf{v}_{ideal}(\phi,\theta,0,1)$ as the columns of the matrix $V_{ideal}{}'$ in (52) for 324 different combinations of ϕ and θ. Since two polarizations are considered, the total number of calibration points is 648. The matrix V_{ideal} in (52) is then a 180×648 matrix containing the ideal signal vectors for the reduced discretization scheme and the 648 calibration points.

The popular MUltiple SIgnal Classification (MUSIC) algorithm, described in [100–102], is employed here to perform DOA estimation in a polarization diverse scenario. By the theory of this paper, the MUSIC DOA spectrum can be expressed as

$$P(\phi,\theta)=\frac{1}{\lambda_{\min}\left[(A^HA)^{-1}A^HE_NE_N{}^HA\right]} \tag{66}$$

where

$$A=\tilde{C}[\mathbf{v}_{ideal}(\phi,\theta,1,0)\quad\mathbf{v}_{ideal}(\phi,\theta,0,1)], \tag{67}$$

$\lambda_{\min}[\cdot]$ is the smallest eigenvalue of the matrix inside the brackets, and E_N is the matrix containing the noise eigenvectors obtained through the eigendecomposition of the correlation matrix. A signal scenario involving two plane waves arriving from $(\phi,\theta)=(-30°,60°)$ and $(\phi,\theta)=(0°,45°)$, respectively, is considered. In addition, the two signals are circularly polarized. The first signal is RHCP, i.e., $(E_\theta,E_\phi)=(j,1)$, whereas the second signal is LHCP, i.e., $(E_\theta,E_\phi)=(1,j)$. The eigenvalue decomposition of the correlation matrix provides six noise eigenvectors, which are associated with the six smallest eigenvalues, to fill the matrix E_N in (66). The 2-D DOA spectra are presented in Figure 10.

For comparison, the DOA spectra obtained without compensation, with a square coupling matrix having dimensions 8×8 and with the full 8×5950 matrix, are also shown. The accuracies and resolutions obtained with the larger matrices in Figure 10c and d are seen to be significantly better. The reduced 8×180 matrix is seen to be a very reasonable compromise with a slight performance degradation but a reduction of approximately 97% of the memory requirement and computations required for the evaluation of the DOA spectra.

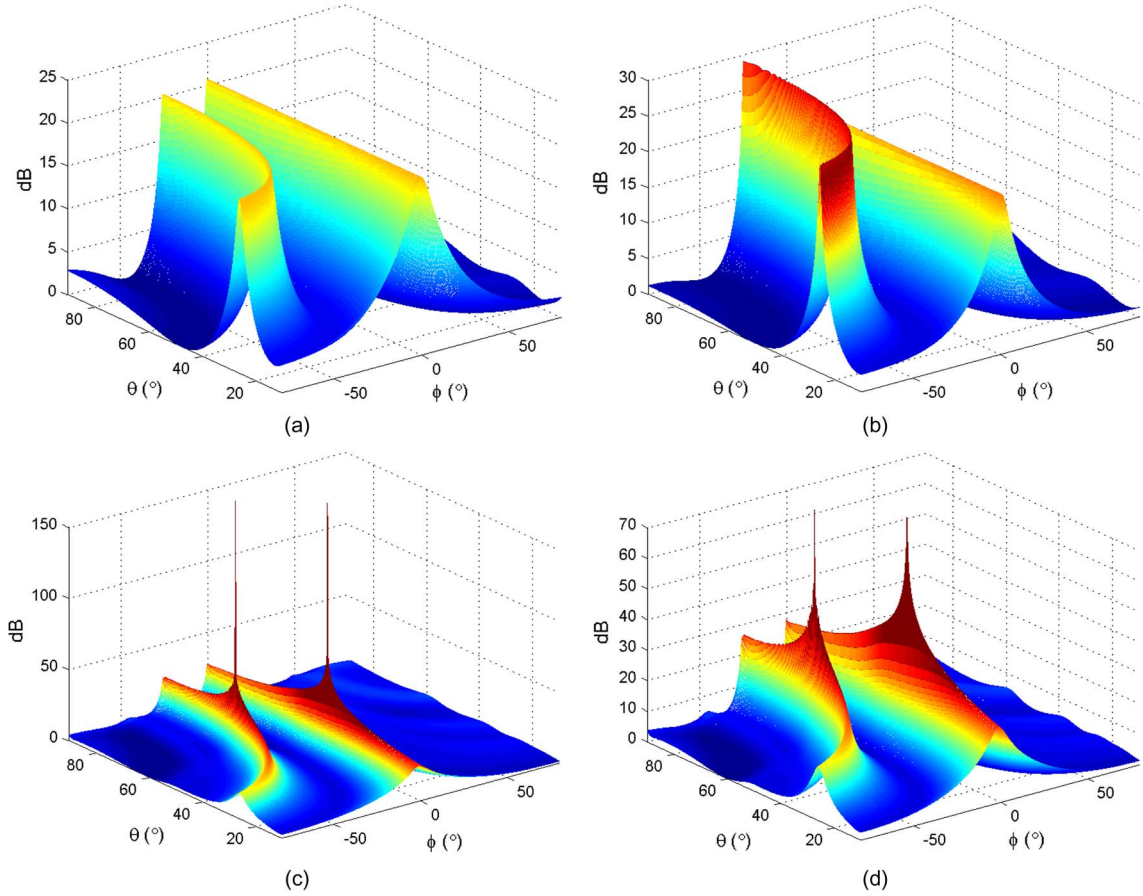

Figure 10. 2-D DOA estimation using the eight-dipole linear array in front of a rectangular conducting plate for two circularly polarized signals from $(\phi, \theta) = (-30^\circ, 60^\circ)$ and $(0^\circ, 45^\circ)$ using MUSIC. Mutual coupling compensation implemented with an 8×180 coupling matrix estimate is seen to give very satisfying performance and efficiency with sharp peaks toward the two signals.

It is important to note here that the 8×180 $\tilde{C}$ matrix can also be determined with measurements using (51), where the matrix V is filled with measured steering vectors. In the case studied in this section, 648 measured steering vectors are necessary to obtain $\tilde{C}$. This is a substantial reduction compared with the number of measurements required for 2-D operation using conventional means. More details on this are available in [89].

6. Conclusion

This paper has thoroughly reviewed the limitations of current mutual coupling compensation methods. Through the derivation of clear theoretical foundations that apply to both receive and transmit systems, the theory of mutual coupling compensation was unified to provide efficient mutual coupling compensation methods that can be employed with systems of arbitrary geometries. Reciprocity relationships were clearly derived based on the receive and transmit formulations, thereby allowing the use of receive-mode compensation data for both reception and transmission if the reciprocity relationships are employed properly. Both theoretical and experimental techniques can be used to evaluate mutual coupling by the presented theory. This theory can be verified in a straightforward fashion using proven electromagnetic codes, and the examples given in this paper on retrodirective systems, beamformers, and DOA estimation can be followed by the reader for validation. Finally, this theory will likely find several other applications than those presented and contributes to the areas of antenna theory, mutual coupling analysis, complex structure modeling, and antenna measurements.

7. Appendix
Derivation of Analytical Formulations in Table 1

The analytical formulations presented in Table 1 are better understood using the various equivalent circuits of antenna systems shown in Figure 11. In receive-mode, the open-circuit voltages are given by

$$\mathbf{v}_{oc_A} = -Z_{ANT} I^T \mathbf{v}_{ideal} \tag{68}$$

$$\mathbf{v}_{oc_L} = -(Z_L + Z) I_L^T \mathbf{v}_{ideal} \tag{69}$$

$$\mathbf{v}_{oc} = -Z I_{sc}^T \mathbf{v}_{ideal}. \tag{70}$$

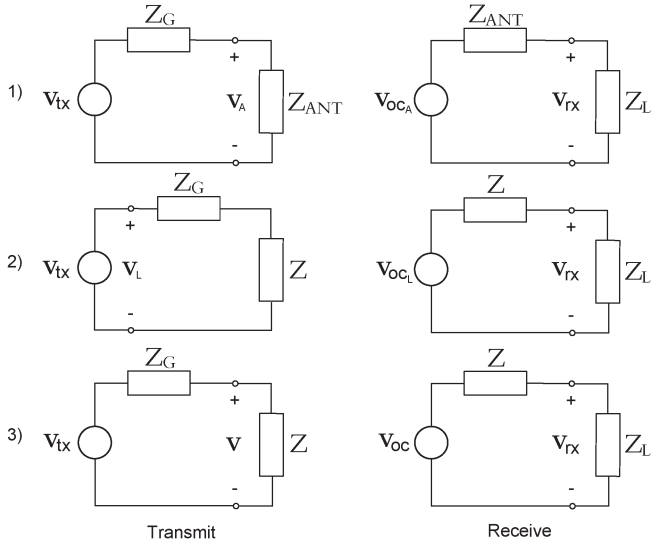

Figure 11. Equivalent circuits of (left) transmit and (right) receive antenna systems for the three different loading conditions given in Table 1. These equivalent circuits use vectors and matrices to represent voltages and impedances.

This is consistent with classic antenna theory presented in [6]. The port voltages should be equal, irrespective of the method. By circuit theory, these are given by

$$\mathbf{v}_{rx} = Z_L(Z_L + Z_{ANT})^{-1}\mathbf{v}_{oc_A} \quad (71)$$
$$= Z_L(Z_L + Z)^{-1}\mathbf{v}_{oc_L} \quad (72)$$
$$= Z_L(Z_L + Z)^{-1}\mathbf{v}_{oc}. \quad (73)$$

Substituting (68)–(70) into (71)–(73) and performing some matrix manipulations gives

$$\mathbf{v}_{rx} = -Z_L(Z_L + Z_{ANT})^{-1}Z_{ANT}I^T\mathbf{v}_{ideal} \quad (74)$$
$$= -Z_L I_L^T\mathbf{v}_{ideal} \quad (75)$$
$$= -Z_L(Z_L + Z)^{-1}ZI_{sc}^T\mathbf{v}_{ideal}. \quad (76)$$

The admittance formulations are obtained by substituting $Z_L = {Y_L}^{-1}$, $Z_{ANT} = {Y_{ANT}}^{-1}$, and $Z = Y^{-1}$ into (74)–(76). For example, (76) gives

$$\begin{aligned}\mathbf{v}_{rx} &= -Y_L^{-1}\left(Y_L^{-1} + Y^{-1}\right)^{-1}Y^{-1}I_{sc}^T\mathbf{v}_{ideal} \\ &= -Y_L^{-1}Y_L(Y_L + Y)^{-1}YY^{-1}I_{sc}^T\mathbf{v}_{ideal} \\ &= -(Y_L + Y)^{-1}I_{sc}^T\mathbf{v}_{ideal}. \quad (77)\end{aligned}$$

In transmit-mode, the radiated fields are scaled by $\mathbf{v}_A$, $\mathbf{v}_L$, and $\mathbf{v}$, which are obtained by voltage division in 1) and 3). In 2), $\mathbf{v}_L$ is simply equal to $\mathbf{v}_{tx}$. The admittance formulations in transmit-mode are obtained in the same fashion as the example of (77).

8. References

[1] H. S. Lui, H. T. Hui, and M. S. Leong, "A note on the mutual coupling problems in transmitting and receiving antenna arrays," *IEEE Antennas Propag. Mag.*, vol. 51, no. 5, pp. 171–176, Oct. 2009.

[2] C. A. Balanis, *Antenna Theory: Analysis and Design*, 2nd ed. New York, NY, USA: Wiley, 1997.

[3] R. C. Hansen, *Phased Array Antennas*. New York, NY, USA: Wiley, 1998.

[4] T. A. Milligan, *Modern Antenna Design*, 2nd ed. New York, NY, USA: Wiley, 2005.

[5] R. J. Mailloux, *Phased Array Antenna Handbook*, 2nd ed. Boston, MA, USA: Artech House, 2005.

[6] S. A. Schelkunoff and H. T. Friis, *Antennas: Theory and Practice*. New York, NY, USA: Wiley, 1952.

[7] R. P. Meys, "A summary of the transmitting and receiving properties of antennas," *IEEE Antennas Propag. Mag.*, vol. 42, no. 3, pp. 49–53, Jun. 2000.

[8] S. Henault, "Evaluation of electromagnetic coupling in antenna systems: A unified theory and its applications," Ph.D. dissertation, Dept. Elect. Comput. Eng., Royal Military College of Canada, Kingston, ON, Canada, Jan. 2012.

[9] S. Henault, Y. M. M. Antar, S. Rajan, R. Inkol, and S. Wang, "The multiple antenna induced EMF method for the precise calculation of the coupling matrix in a receiving antenna array," *Progr. Electromagn. Res. M*, vol. 8, pp. 103–118, 2009.

[10] P. S. Carter, "Circuit relations in radiating systems and applications to antenna problems," *Proc. IRE*, vol. 20, no. 6, pp. 1004–1041, Jun. 1932.

[11] H. E. King, "Mutual impedance of unequal length antennas in echelon," *IRE Trans. Antennas Propag.*, vol. AP-5, no. 3, pp. 306–313, Jul. 1957.

[12] J. H. Richmond and N. H. Geary, "Mutual impedance of nonplanar-skew sinusoidal dipoles," *IEEE Trans. Antennas Propag.*, vol. AP-23, no. 3, pp. 412–414, May 1975.

[13] J. D. Kraus, *Antennas*, 2nd ed. New York, NY, USA: McGraw-Hill, 1988.

[14] S. A. Mitilineos, C. A. Papagianni, G. I. Verikaki, and C. N. Capsalis, "Design of switched beam planar arrays using the method of genetic algorithms," *Progr. Electromagn. Res.*, vol. 46, pp. 105–126, 2004.

[15] A. W. Love, "Comment: On the equivalent circuit of a receiving antenna," *IEEE Antennas Propag. Mag.*, vol. 44, no. 5, pp. 124–125, Oct. 2002.

[16] J. B. Andersen and R. G. Vaughan, "Transmitting, receiving, and scattering properties of antennas," *IEEE Antennas Propag. Mag.*, vol. 45, no. 4, pp. 93–98, Aug. 2003.

[17] J. Van Bladel, "On the equivalent circuit of a receiving antenna," *IEEE Antennas Propag. Mag.*, vol. 44, no. 1, pp. 164–165, Feb. 2002.

[18] R. E. Collin, "Limitations on the Thevenin and Norton equivalent circuits for a receiving antenna," *IEEE Antennas Propag. Mag.*, vol. 45, no. 2, pp. 119–124, Apr. 2003.

[19] C. T. Tai, "A Critical study of the circuit relations of two distant antennas," *IEEE Antennas Propag. Mag.*, vol. 44, no. 6, pp. 32–37, Dec. 2002.

[20] C. T. Tai, "Correction—A critical study of the circuit relations of two distant antennas," *IEEE Antennas Propag. Mag.*, vol. 45, no. 1, p. 125, Feb. 2003.

[21] A. W. Love, "Correction—A critical study of the circuit relations of two distant antennas," *IEEE Antennas Propag. Mag.*, vol. 45, no. 2, p. 42, Apr. 2003.

[22] C. G. Montgomery, R. H. Dicke, and E. M. Purcell, *Principles of Microwave Circuits*. New York, NY, USA: McGraw-Hill, 1948.

[23] S. Ramo and J. Whinnery, *Fields and Waves in Modern Radio*, 2nd ed. New York, NY, USA: Wiley, 1953.

[24] S. Silver, *Microwave Antenna Theory and Design*. New York, NY, USA: McGraw-Hill, 1949.

[25] R. C. Hansen, "Relationships between antennas as scatterers and as radiators," *Proc. IEEE*, vol. 77, no. 5, pp. 659–662, May 1989.

[26] C. C. Su, "On the equivalent generator voltage and generator internal impedance for receiving antennas," *IEEE Trans. Antennas Propag.*, vol. 51, no. 2, pp. 279–285, Feb. 2003.

[27] S. R. Best and B. C. Kaanta, "A tutorial on the receiving and scattering properties of antennas," *IEEE Antennas Propag. Mag.*, vol. 51, no. 5, pp. 26–37, Oct. 2009.

[28] J. W. Wallace and R. Mehmood, "On the accuracy of equivalent circuit models for multi-antenna systems," *IEEE Trans. Antennas Propag.*, vol. 60, no. 2, pp. 540–547, Feb. 2012.

[29] D. M. Pozar, "The active element pattern," *IEEE Trans. Antennas Propag.*, vol. 42, no. 8, pp. 1176–1178, Aug. 1994.

[30] D. F. Kelley and W. L. Stutzman, "Array antenna pattern modeling methods that include mutual coupling effects," *IEEE Trans. Antennas Propag.*, vol. 41, no. 12, pp. 1625–1632, Dec. 1993.
[31] K. Takamizawa, "Analysis of highly coupled wideband antenna arrays using scattering parameter network models," Ph.D. dissertation, Dept. Elect. Comput. Eng., Virginia Polytech. Inst. State Univ., Blacksburg, VA, USA, Dec. 2002.
[32] D. M. Pozar, "A relation between the active input impedance and the active element pattern of a phased array," *IEEE Trans. Antennas Propag.*, vol. 51, no. 9, pp. 2486–2489, Sep. 2003.
[33] D. F. Kelley, "Relationships between active element patterns and mutual impedance matrices in phased array antennas," in *Proc. IEEE Int. Symp. Antennas Propag.*, 2002, pp. 524–527.
[34] D. F. Kelley, "Embedded element patterns and mutual impedance matrices in the terminated phased array environment," in *Proc. IEEE Int. Symp. Antennas Propag.*, 2005, pp. 659–662.
[35] R. F. Harrington, "Antenna excitation for maximum gain," *IEEE Trans. Antennas Propag.*, vol. AP-13, no. 6, pp. 896–903, Nov. 1965.
[36] H. Rogier and E. Bonek, "Analytical spherical-mode-based compensation of mutual coupling in uniform circular arrays for direction-of-arrival estimation," *Int. J. Electron. Commun.*, vol. 60, no. 3, pp. 179–189, Mar. 2006.
[37] A. T. De Hoop, "The N-port receiving antenna and its equivalent electrical network," *Philips Res. Rep.*, vol. 30, pp. 302–315, 1975.
[38] P. S. Kildal, "Equivalent circuits of receive antennas in signal processing arrays," *Microw. Opt. Technol. Lett.*, vol. 21, no. 4, pp. 244–246, May 1999.
[39] K. F. Warnick, B. Woestenburg, L. Belostotski, and P. Russer, "Minimizing the noise penalty due to mutual coupling for a receiving array," *IEEE Trans. Antennas Propag.*, vol. 57, no. 6, pp. 1634–1644, Jun. 2009.
[40] R. O. Schmidt, "Multilinear array manifold interpolation," *IEEE Trans. Signal Process.*, vol. 40, no. 4, pp. 857–866, Apr. 1992.
[41] A. J. Weiss and B. Friedlander, "Manifold interpolation for diversely polarized arrays," *Proc. Inst. Elect. Eng.—Radar, Sonar Navig.*, vol. 141, no. 1, pp. 19–24, Feb. 1994.
[42] R. J. Allard and D. H. Werner, "The model-based parameter estimation of antenna radiation patterns using windowed interpolation and spherical harmonics," *IEEE Trans. Antennas Propag.*, vol. 51, no. 8, pp. 1891–1906, Aug. 2003.
[43] M. Landmann and G. Del Galdo, "Efficient antenna description for MIMO channel modelling and estimation," in *Proc. 7th Eur. Conf. Wireless Technol.*, Amsterdam, The Netherlands, 2004, pp. 217–220.
[44] G. Del Galdo, J. Lotze, M. Landmann, and M. Haardt, "Modelling and manipulation of polarimetric antenna beam patterns via spherical harmonics," in *Proc. 14th Eur. Signal Process. Conf.*, Florence, Italy, Sep. 2006, pp. 1–5.
[45] F. Belloni, A. Richter, and V. Koivunen, "DoA estimation via manifold separation for arbitrary array structures," *IEEE Trans. Signal Process.*, vol. 55, no. 10, pp. 4800–4810, Oct. 2007.
[46] H. T. Hui, "Decoupling methods for the mutual coupling effect in antenna arrays: A review," *Recent Patents Eng.*, vol. 1, no. 2, pp. 187–193, Jun. 2007.
[47] T. Su and H. Ling, "On modeling mutual coupling in antenna arrays using the coupling matrix," *Microw. Opt. Technol. Lett.*, vol. 28, no. 4, pp. 231–237, Feb. 2001.
[48] P. Darwood, P. N. Fletcher, and G. S. Hilton, "Mutual coupling compensation in small planar array antennas," *Proc. Inst. Elect. Eng.—Microw., Antennas Propag.*, vol. 145, no. 1, pp. 1–6, Feb. 1998.
[49] H. Steyskal and J. S. Herd, "Mutual coupling compensation in small array antennas," *IEEE Trans. Antennas Propag.*, vol. 38, no. 12, pp. 1971–1975, Dec. 1990.
[50] I. J. Gupta and A. A. Ksienski, "Effect of mutual coupling on the performance of adaptive arrays," *IEEE Trans. Antennas Propag.*, vol. AP-31, no. 5, pp. 785–791, Sep. 1983.
[51] C. C. Yeh, M. L. Leou, and D. R. Ucci, "Bearing estimations with mutual coupling present," *IEEE Trans. Antennas Propag.*, vol. 37, no. 10, pp. 1332–1335, Oct. 1989.
[52] C. Roller and W. Wasylkiwskyj, "Effects of mutual coupling on super-resolution DF in linear arrays," in *Proc. IEEE Int. Conf. Acoust., Speech, Signal Process.*, vol. 5, 1992, pp. 257–260.
[53] Z. Huang, C. A. Balanis, and C. R. Birtcher, "Mutual coupling compensation in UCAs: Simulations and experiment," *IEEE Trans. Antennas Propag.*, vol. 54, no. 11, pp. 3082–3086, Nov. 2006.
[54] K. C. Lee and T. H. Chu, "A circuit model for mutual coupling analysis of a finite antenna array," *IEEE Trans. Electromagn. Compat.*, vol. 38, no. 3, pp. 483–489, Aug. 1996.
[55] K. W. Lo and T. B. Vu, "Simple S-parameter model for receiving antenna array," *Electron. Lett.*, vol. 24, no. 20, pp. 1264–1266, Sep. 1988.
[56] K. M. Pasala and E. M. Friel, "Mutual coupling effects and their reduction in wideband direction of arrival estimation," *IEEE Trans. Aerosp. Electron. Syst.*, vol. 30, no. 4, pp. 1116–1122, Apr. 1994.
[57] R. S. Adve and T. K. Sarkar, "Compensation for the effects of mutual coupling on direct data domain adaptive algorithms," *IEEE Trans. Antennas Propag.*, vol. 48, no. 1, pp. 86–94, Jan. 2000.
[58] R. F. Harrington, *Field Computation by Moment Methods*. New York, NY, USA: Wiley, 1968.
[59] J. Pierre and M. Kaveh, "Experimental performance of calibration and direction-finding algorithms," in *Proc. IEEE Int. Conf. Acoust., Speech, Signal Process.*, vol. 2, Toronto, ON, Canada, Apr. 1991, pp. 1365–1368.
[60] T. Su, K. Dandekar, and H. Ling, "Simulation of mutual coupling effect in circular arrays for direction-finding applications," *Microw. Opt. Technol. Lett.*, vol. 26, no. 5, pp. 331–336, Sep. 2000.
[61] K. R. Dandekar, H. Ling, and G. Xu, "Experimental study of mutual coupling compensation in smart antenna applications," *IEEE Trans. Wireless Commun.*, vol. 1, no. 3, pp. 480–487, Jul. 2002.
[62] H. T. Hui, "Reducing the mutual coupling effect in adaptive nulling using a re-defined mutual impedance," *IEEE Microw. Wireless Compon. Lett.*, vol. 12, no. 5, pp. 178–180, May 2002.
[63] H. T. Hui, "Compensating for the mutual coupling effect in direction finding based on a new calculation method for mutual impedance," *IEEE Antennas Wireless Propag. Lett.*, vol. 2, no. 1, pp. 26–29, 2003.
[64] H. T. Hui, "Improved compensation for the mutual coupling effect in a dipole array for direction finding," *IEEE Trans. Antennas Propag.*, vol. 51, no. 9, pp. 2498–2503, Sep. 2003.
[65] H. T. Hui, "A practical approach to compensate for the mutual coupling effect in an adaptive dipole array," *IEEE Trans. Antennas Propag.*, vol. 52, no. 5, pp. 1262–1269, May 2004.
[66] H. T. Hui, "A new definition of mutual impedance for application in dipole receiving antenna arrays," *IEEE Antennas Wireless Propag. Lett.*, vol. 3, no. 1, pp. 364–367, Dec. 2004.
[67] S. Henault and Y. M. M. Antar, "Wideband analysis of mutual coupling compensation methods," *Int. J. Antennas Propag.*, vol. 2011, 2011, Art. ID. 756 153.
[68] B. Friedlander and A. J. Weiss, "Direction finding in the presence of mutual coupling," *IEEE Trans. Antennas Propag.*, vol. 39, no. 3, pp. 273–284, Mar. 1991.
[69] E. K. L. Hung, "A critical study of a self-calibrating direction-finding method for arrays," *IEEE Trans. Signal Process.*, vol. 42, no. 2, pp. 471–474, Feb. 1994.
[70] F. S. Sellone and A. Serra, "A novel online mutual coupling compensation algorithm for uniform and linear arrays," *IEEE Trans. Signal Process.*, vol. 55, no. 2, pp. 560–573, Feb. 2007.
[71] M. Lin and L. Yang, "Blind calibration and DOA estimation with uniform circular arrays in the presence of mutual coupling," *IEEE Antennas Wireless Propag. Lett.*, vol. 5, no. 1, pp. 315–318, Dec. 2006.
[72] D. Y. Gao, B. H. Wang, and Y. Guo, "Comments on 'Blind calibration and DOA estimation with uniform circular arrays in the presence of mutual coupling'," *IEEE Antennas Wireless Propag. Lett.*, vol. 5, no. 1, pp. 566–568, Dec. 2006.
[73] M. Lin and L. Yang, "Reply to the comments on 'Blind calibration and DOA estimation with uniform circular arrays in the presence of mutual coupling'," *IEEE Antennas Wireless Propag. Lett.*, vol. 5, no. 1, pp. 568–569, Dec. 2006.
[74] Q. Bao, C. C. Ko, and W. Zhi, "DOA estimation under unknown mutual coupling and multipath," *IEEE Trans. Aerosp. Electron. Syst.*, vol. 41, no. 2, pp. 565–573, Apr. 2005.
[75] Z. Ye and C. Liu, "On the resiliency of MUSIC direction finding against antenna sensor coupling," *IEEE Trans. Antennas Propag.*, vol. 56, no. 2, pp. 371–380, Feb. 2008.
[76] Z. Ye and C. Liu, "2-D DOA estimation in the presence of mutual coupling," *IEEE Trans. Antennas Propag.*, vol. 56, no. 10, pp. 3150–3158, Oct. 2008.
[77] Y. Zhang, Q. Wan, and A. M. Huang, "Localization of narrow band sources in the presence of mutual coupling via sparse solution finding," *Progr. Electromagn. Res.*, vol. 86, pp. 243–257, 2008.
[78] T. Svantesson, "Antennas and propagation from a signal processing perspective," Ph.D. dissertation, Dept. Signals Syst., Chalmers Univ. Technol., Göteborg, Sweden, 2001.
[79] S. Henault and Y. M. M. Antar, "Limitations of online calibration methods," in *Proc. IEEE Int. Symp. Antennas Propag.*, Toronto, ON, Canada, Jul. 2010, pp. 1–4.
[80] I. J. Gupta et al., "An experimental study of antenna array calibration," *IEEE Trans. Antennas Propag.*, vol. 51, no. 3, pp. 664–667, Mar. 2003.
[81] C. K. E. Lau, R. S. Adve, and T. K. Sarkar, "Minimum norm mutual coupling compensation with applications in direction of arrival estimation," *IEEE Trans. Antennas Propag.*, vol. 52, no. 8, pp. 2034–2041, Aug. 2004.

[82] Q. Y. Yuan, Q. Chen, and K. Sawaya, "Accurate DOA estimation using array antenna with arbitrary geometry," *IEEE Trans. Antennas Propag.*, vol. 53, no. 4, pp. 1352–1357, Apr. 2005.
[83] S. Henault, Y. M. M. Antar, S. Rajan, R. Inkol, and S. Wang, "Effects of mutual coupling on the accuracy of adcock direction finding systems," *IEEE Trans. Aerosp. Electron. Syst.*, vol. 48, no. 4, pp. 2990–3005, Oct. 2012.
[84] T. Su and H. Ling, "On the simultaneous modeling of array mutual coupling and array-platform interactions," *Microw. Opt. Technol. Lett.*, vol. 33, no. 3, pp. 167–171, May 2002.
[85] A. Ferreol, E. Boyer, P. Larzabal, and M. Haardt, "On the introduction of an extended coupling matrix for a 2D bearing estimation with an experimental RF system," *Signal Process.*, vol. 87, no. 9, pp. 2005–2016, Sep. 2007.
[86] J. B. Andersen and H. H. Rasmussen, "Decoupling and descattering networks for antennas," *IEEE Trans. Antennas Propag.*, vol. AP-24, no. 6, pp. 841–846, Nov. 1976.
[87] M. Kragalott, M. S. Kluskens, D. A. Zolnick, W. M. Dorsey, and J. A. Valenzi, "A toolset independent hybrid method for calculating antenna coupling," *IEEE Trans. Antennas Propag.*, vol. 59, no. 2, pp. 443–451, Feb. 2011.
[88] A. E. H. Love, "The integration of equations of propagation of electric waves," *Philos. Trans. Roy. Soc. London A, Math. Phys. Sci.*, vol. 197, pp. 1–45, 1901.
[89] S. Henault, S. K. Podilchak, S. M. Mikki, and Y. M. M. Antar, "A methodology for mutual coupling estimation and compensation in antennas," *IEEE Trans. Antennas Propag.*, vol. 61, no. 3, pp. 1119–1131, Mar. 2013.
[90] S. Henault and Y. M. M. Antar, "On the interpolation of radiation patterns in the calibration of antenna arrays," in *IEEE Int. Symp. Antennas Propag.*, Spokane, WA, USA, Jul. 2011, pp. 1747–1750.
[91] S. Henault and Y. M. M. Antar, "A hybrid approach for antenna array calibration," in *Proc. IEEE Int. Symp. Antennas Propag.*, Spokane, WA, USA, Jul. 2011, pp. 1751–1754.
[92] C. Pon, "Retrodirective array using the heterodyne technique," *IEEE Trans. Antennas Propag.*, vol. 12, no. 2, pp. 176–180, Mar. 1964.
[93] A. F. Kay, "Comments on self-phasing array antennas and electronically adaptive antenna systems," *IEEE Trans. Antennas Propag.*, vol. AP-12, no. 6, pp. 792–793, Nov. 1964.
[94] V. F. Fusco, "Response of retrodirective array in the presence of multiple spatially separated sources," *IEEE Trans. Antennas Propag.*, vol. 54, no. 4, pp. 1352–1354, Apr. 2006.
[95] *NEC-2 Manual*, Lawrence Livermore National Laboratory, Livermore, CA , USA, 1996.
[96] L. C. Van Atta, "Electromagnetic reflector," U.S. Patent 2 908 002, Oct. 6, 1959.
[97] T. Larsen, "Reflector arrays," *IEEE Trans. Antennas Propag.*, vol. AP-14, no. 6, pp. 689–693, Nov. 1966.
[98] J. Appel-Hansen, "A van Atta reflector consisting of half-wave dipoles," *IEEE Trans. Antennas Propag.*, vol. AP-14, no. 6, pp. 694–700, Nov. 1966.
[99] FEKO-Comprehensive EM Solutions. [Online]. Available: http://www.feko.info
[100] R. O. Schmidt, "Multiple emitter location and signal parameter estimation," *IEEE Trans. Antennas Propag.*, vol. AP-34, no. 3, pp. 276–280, Mar. 1986.
[101] R. O. Schmidt and R. Franks, "Multiple source DF signal processing: An experimental system," *IEEE Trans. Antennas Propag.*, vol. AP-34, no. 3, pp. 281–290, Mar. 1986.
[102] E. R. Ferrara and T. M. Parks, "Direction finding with an array of antennas having diverse polarizations," *IEEE Trans. Antennas Propag.*, vol. AP-31, no. 2, pp. 231–236, Mar. 1983.

Simon Henault received the B.Eng. degree from Laval University, Québec City, QC, Canada, in 2001 and the M.A.Sc. and Ph.D. degrees from the Royal Military College of Canada, Kingston, ON, Canada, in 2008 and 2012, respectively, all in electrical engineering.

Since 1998, he has been with Canada's Department of National Defence in various capacities, including two years as a faculty member with the Royal Military College of Canada and multiple assignments with Defence Research and Development Canada. He has expertise in antenna, radio frequency and signal processing systems employed in a variety of electronic warfare, space communication, and unmanned aerial vehicle platforms.

Dr. Henault is a regular Reviewer for several journals and conferences.

Yahia M. M. Antar (S'73–M'76–SM'85–LF'00) received the B.Sc. (Hons.) degree from Alexandria University, Alexandria, Egypt, in 1966 and the M.Sc. and Ph.D. degrees from the University of Manitoba, Winnipeg, MB, Canada, in 1971 and 1975, respectively, all in electrical engineering.

In 1977, he held a Government of Canada Visiting Fellowship with the Communications Research Centre, Ottawa, ON, Canada, where he worked with the Space Technology Directorate on communications antennas for satellite systems. In May 1979, he joined the Division of Electrical Engineering, National Research Council of Canada, Ottawa, where he worked on polarization radar applications in remote sensing of precipitation, radio wave propagation, electromagnetic scattering, and radar cross-section investigations. In November 1987, he joined the staff of the Department of Electrical and Computer Engineering, Royal Military College of Canada, Kingston, ON, where he has held the position of Professor since 1990 and is currently the Vice Dean for defense and security research. He has authored or coauthored about 200 journal papers, many chapters in books, and about 400 refereed conference papers, holds several patents, has chaired several national and international conferences, and has given plenary talks at many conferences. He has supervised and cosupervised over 80 Ph.D. and M.Sc. theses at the Royal Military College of Canada and at Queen's University, Kingston, several of which have received the Governor General of Canada Gold Medal, the outstanding Ph.D. thesis of the Division of Applied Science, as well as many Best Paper Awards in major international symposia. He served as the Chairman of the Canadian National Commission for Radio Science (CNC, URSI, 1999–2008) and the Commission B National Chair (1993–1999) and held an adjunct appointment at the University of Manitoba and has a cross appointment at Queen's University.

Dr. Antar is a Fellow of the Engineering Institute of Canada and the Electromagnetic Academy. He serves as an Associate Editor for the IEEE ANTENNAS AND PROPAGATION MAGAZINE, served as an Associate Editor for the IEEE TRANSACTIONS ON ANTENNAS AND PROPAGATION and the IEEE ANTENNAS AND WIRELESS PROPAGATION LETTERS, and was a member of the Editorial Board of the International Journal of RF and Microwave Computer-Aided Engineering. He served on Natural Sciences and Engineering Research Council of Canada grant selection and strategic grant committees, on Ontario Early Research Awards panels, and on review panels for the National Science Foundation. In May 2002, he was awarded a Tier 1 Canada Research Chair in Electromagnetic Engineering, which has been renewed in 2009. In 2003, he was awarded the Royal Military College of Canada "Excellence in Research" Prize, and the RMCC Class of 1965 Teaching Excellence Award in 2012. He was elected by the Council of the International Union of Radio Science to the Board as Vice President in August 2008 and in 2013 and to the IEEE Antennas and Propagation Society Administration Committee in December 2009. On January 31, 2011, he was appointed Member of the Canadian Defence Science Advisory Board. He is on the IEEE Antennas and Propagation Society Distinguished Lecturers Program. In October 2012, he received the Queen's Diamond Jubilee Medal from the Governor General of Canada in recognition of his contribution to Canada. He was a recipient of the 2014 IEEE Canada RA Fessenden Silver Medal and the 2015 IEEE Canada J. M. Ham Outstanding Engineering Education Award.